The paleoceanography of Kattegat during the last deglaciation from benthic foraminiferal stable isotopes

Yasmin Bokhari Friberg

Dissertations in Geology at Lund University,
Master's thesis, no 461
(45 hp/ECTS credits)

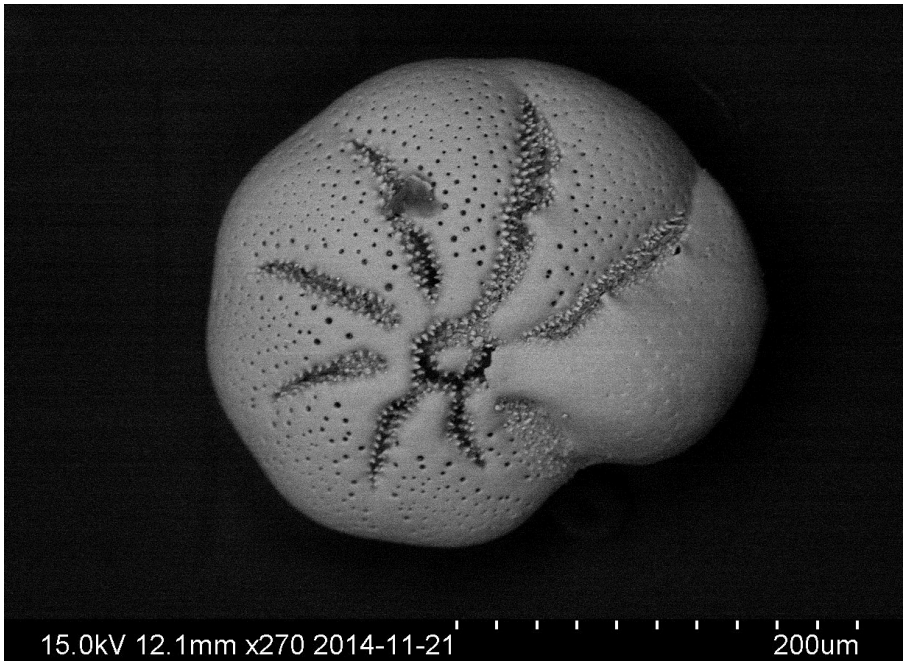

Department of Geology
Lund University
2015

The paleoceanography of Kattegat during the last deglaciation from benthic foraminiferal stable isotopes

Master's thesis

Yasmin Bokhari Friberg

Department of Geology
Lund University
2015

Contents

Cover Picture: SEM image of *Elphidium excavatum*. Photo by Nadine B. Quintana Krupinski, 2015.

The paleoceanography of Kattegat during the last deglaciation from benthic foraminiferal stable isotopes

YASMIN BOKHARI FRIBERG

Bokhari Friberg, Y., 2015: The paleoceanography of Kattegat during the last deglaciation from benthic foraminiferal stable isotopes. *Dissertations in Geology at Lund University*, No. 461, 30 pp. 45 hp (45 ECTS credits).

Abstract: This thesis is based on a sediment record collected from the Kattegat Sea, southwestern Scandinavia (Anholt Island area) during IODP Expedition 347 in autumn 2013, and focuses on a portion of this record spanning ~18—14 thousand years ago (ka BP), representing the last deglaciation at the end of the Weichselian. Benthic foraminifera of the species *Elphidium excavatum clavatum* were analysed for stable isotopes ($\delta^{18}O$ and $\delta^{13}C$) to reconstruct the paleoenvironment and oceanographic setting, such as bottom water salinity, temperature and ventilation. Additionally, the sediment coarse fraction (>63µm) and mean weight per foraminifera shell were measured as a complement to the isotope analyses to interpret other factors, such as sediment origin and conditions at the seafloor. $\delta^{18}O$ was used to calculate paleosalinities in Kattegat bottom waters by assuming a temperature between 0 and 4°C. These calculations yielded salinities varying between 13 and 27, with a rapid freshening at the beginning of the record, and a subsequent slower, stepwise salinity decrease, followed by a rise in salinity after 15.7 ka. Very negative $\delta^{13}C$ values suggest a strong stratification between fresh surface and saline bottom waters, likely due to large amounts of glacial meltwater discharging into the Kattegat as the Scandinavian Ice Sheet (SIS) melted. The $\delta^{13}C$ values increase after 15.7 ka, suggesting a weakened stratification, perhaps due to stronger seawater influence. A simultaneous decline in average foraminifera shell weight suggests worse calcification conditions for *Elphidium excavatum* in Kattegat bottom waters. Percent coarse sediment data shows a high amount of sand size fraction at the very beginning of the record, but very low values between ~18 and 15.7 ka, suggesting that Anholt was situated close to the ice margin at 18 ka, but saw a retreat of the SIS during the subsequent few thousand years.

Keywords: paleoceanography, deglaciation, foraminifera, stable isotopes, Baltic Sea, Kattegat, $\delta^{18}O$, $\delta^{13}C$

Supervisor(s): Helena L. Filipson, Nadine B. Quintana Krupinski

Subject: Quaternary Geology

Yasmin Bokhari Friberg, Department of Geology, Lund University, Sölvegatan 12, SE-223 62 Lund, Sweden. E-mail: aar08ybo@student.lu.se

Paleoceanografi i Kattegatt under den senaste deglaciationen från bentiska foraminiferers stabila isotoper

YASMIN BOKHARI FRIBERG

Bokhari Friberg, Y., 2015: Paleoceanografi i Kattegat under den senaste deglaciationen från bentiska foraminiferers stabila isotoper. *Examensarbeten i geologi vid Lunds Universitet*, Nr. 461, 30 sid. 45 hp.

Sammanfattning: En borrkärna från Anholt (Kattegatt) togs upp under IODP-expedition 347 i Östersjön. Kärnan är daterad till ~18-14 ka BP och representerar deglaciationen i slutet av Weichselistiden. Bentiska foraminiferer av arten *Elphidium excavatum clavatum* analyserades för stabila isotoper ($\delta^{18}O$ och $\delta^{13}C$) för att rekonstruera regionens paleoklimat och paleoceanografi, såsom salinitet, ventilation och produktivitet i bottenvattnet. Sedimentets grovkorniga fraktion (> 63µm) mättes även, samt medelvikten per foraminiferskal, för att kunna tolka andra faktorer, såsom sedimentets ursprung och förhållanden i foraminiferernas livsmiljö. $\delta^{18}O$ användes för att beräkna paleosalinitet i Kattegatts bottenvattnet genom att anta en temperatur mellan 0 och 4°C. Dessa beräkningar gav salthalter mellan 13 och 27, med en snabb minskning i början av kärnan, och sedan en långsammare minskning till 15,7 ka då saliniteten steg. Negativa $\delta^{13}C$-värden indikerar en stark skiktning mellan sött eller bräckt ytvatten och saltare bottenvatten, på grund av stora mängder glacialt smältvatten som släpptes ut i Kattegatt när den skandinaviska inlandsisen drog sig tillbaka. $\delta^{13}C$-värden ökar vid 15,7 ka, vilket tyder på en försvagad skiktning och större inflytande av havsvatten från Nordsjön. Samtidigt börjar foraminifernas skalvikt att minska, vilket tyder på sämre kalcifikationsförhållanden för *Elphidium excavatum.* Andelen grovt sediment visar en stor mängd sandkornigt material i början av borrkärnan, men sjunker till värden nära 0 mellan ~18 och 16 ka, vilket tyder på att Anholt var beläget nära iskanten vid 18 ka, varpå isen drog sig tillbaka under de följande ca. 3700 åren som borrkärnan representerar.

Nyckelord: paleoceanografi, deglaciation, foraminiferer, stabila isotoper, Östersjön, Kattegatt, $\delta^{18}O$, δ^{13}

Yasmin Bokhari Friberg, Geologiska institutionen, Lunds Universitet, Sölvegatan 12, SE-223 62 Lund, Sweden. E-mail: aar08ybo@student.lu.se

1 Introduction

1.1 Background

During the end of the Weichselian glacial, Scandinavia experienced numerous retreats and re-advances of the Scandinavian Ice Sheet (SIS), which greatly impacted the environment and oceanography of the region. The geographical position of the Kattegat Sea makes it a key location for paleoenvironmental studies (Larsen et al. 2009).

The Baltic Sea Basin is one of the largest intracontinental shelf seas of the world. Its brackish nature results from a mix of the saline Atlantic waters and the fresh water entering through rivers, rainfall and infiltration. The high sedimentation rate (1-5 m/1000 years) makes high-resolution archive analysis possible. Benthic foraminifera are found in the Baltic Sea and are suitable for paleoenvironmental reconstructions as the geochemistry of their shells can provide important information on environmental factors such as salinity, changes in temperature, productivity and oxygenation.

In autumn 2013, the Integrated Ocean Drilling Program (IODP) conducted a seafloor drilling expedition in the Baltic Sea and Kattegat to retrieve sediment cores with the aim of studying the climatic development during the past glacial-interglacial cycle. The cores previously available were only 20 m or less, and deeper boreholes are necessary in order to be able to discover a more comprehensive and detailed account of the Baltic Sea's history. For this master's thesis, foraminifera from site M0060A (Anholt Loch, southern Kattegat. 56°37.21′N, 11°40.24′E) have been picked, identified and analysed for stable isotopes. Some additional samples have been prepared for radiocarbon dating. The total length of the core studied in this project is 232.5 mbsf (metres below sea floor), and the depths of the presently studied samples range between ~9 and 82 mbsf, which represents approximately 18 – 14 ka BP (thousand years before present), i.e. the most recent deglaciation.

The main questions to be answered are the following:

- How can the deglacial isotope records from the Kattegat be related to global and local climate change?
- Can climate events related to Scandinavian Ice Sheet fluctuations during deglaciation be observed in the Kattegat oxygen and carbon isotope records? For example, can the isotope records show large freshwater discharge events (as salinity changes) during the deglaciation?
- Which environmental conditions can be reconstructed from foraminifera oxygen and carbon isotopes? Are there any significant limitations to these proxies and if so, what can be done to give a better understanding of past climatic events and fluctuations?

1.2 Baltic Sea present

The Baltic Sea Basin is 1500 km long, 650 km wide and consists of several different basins: the Bothnian Bay, Bothnian Sea, Gulf of Finland, Gulf of Riga, Baltic Proper, Belt Sea and Kattegat (Figure 1). The mean depth is 54 m and mostly ranges between 50 and 150 m, although the Landsort Deep drops to 459 m (Zillén et al. 2008). Compared to other intracontinental basins of similar sizes, such as the Black Sea (with a mean depth of 1197 m), the Red Sea (491 m) and the Caspian Sea (211 m), the Baltic is a relatively shallow basin (Leppäranta & Myrberg 2009).

The waters of the Baltic are connected to the Atlantic by three narrow Danish straits: Great Belt, Little Belt and Öresund, where water exchange is limited (Leppäranta & Myrberg 2009). The shallow nature of the Danish straits poses a significant obstacle for saline bottom water from entering the Baltic Sea, leading to a considerable difference in bottom water salinity between the two sides of the straits (~30 in Kattegat versus 12 in the Baltic Proper). The restricted water inflow, coupled with high precipitation rates (400 – 600 mm per year), low evaporation (~460 mm per year) and large discharge from connecting rivers, results in the Baltic Sea having a positive estuarine circulation, or a so-called positive water budget (Voipio 1981).

Rather than being a part of the Baltic Sea, Kattegat is a transition zone between the Baltic and the Atlantic Ocean (Voipio 1981). It is a depression south of Skagerrak, with a maximum depth of 140 m but averaging 26 m (Nordberg 1991), and can be perceived as a branch of the Norwegian Channel, which connects to

Fig. 1. Map of the Baltic Sea, Skagerrak, Kattegat and Anholt, the site from which the sediment core is retrieved.

the North Sea (Larsen et al. 2009). North Sea and Atlantic bottom waters with high salinity (30 – 35) enter Kattegat via Skagerrak, while low salinity waters (8 – 12) enter from the Baltic through the Danish Straits (Nordberg 1991), resulting in a distinct two layer stratification and permanent halocline in Kattegat where the surface has a salinity of 15 – 25 and the bottom waters 30 – 35 (Danielssen et al. 1997). This pronounced stratification of water masses has led to poor ventilation and a permanent oxygen deficiency below the halocline in the Baltic Sea and Kattegat (Voipio 1981).

The amount of saline inflow is mainly governed by frequent deep-water streams from the North Sea. Additionally, Danielssen et al. (1997) recorded that saline surface waters from Skagerrak had a strong inflow into Kattegat during pronounced northwesterly winds at the end of May, causing increased surface salinities and reduced outflow from Kattegat. There is also, albeit to a lesser extent, an outflow of brackish water through the straits. This depends on sea level differences between the Baltic Sea and North Sea and can be strengthened by easterly winds that push fresher water westward along the surface. The straits therefore have a permanent salinity stratification that divides the outflowing brackish surface layer from the denser deep inflowing ocean water (Voipio 1981).

1.3 Baltic Sea past

The climate and environmental conditions in the Baltic Sea area have been strongly controlled by the large ice sheets that covered Scandinavia and northern Europe during the Last Glacial Maximum (LGM) c. 26,500 – 19,000 yr BP (Clark et al. 2009). The deglaciation that followed led to the development of the Baltic Sea in four main stages: the Baltic Ice Lake, the Yoldia Sea, the Ancylus Lake and the Littorina Sea, as it transitioned between freshwater lake and marine environment (Björck 1995). The main changes consist of salinity, productivity, oxygen level and circulation pattern variations due to ice melting, rising and falling sea levels, land uplift and infilling of marine water into the basin (Andrén et al. 2011). The Kattegat area underwent numerous ice advances and retreats during the Weichselian glacial and had its last ice cover ~18 ka BP (Figure 2).

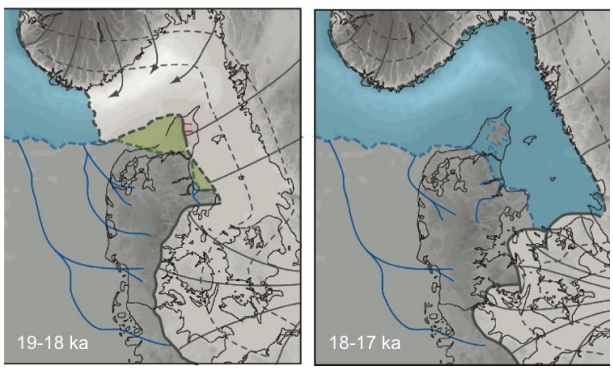

Fig. 2. Kattegat and Skagerrak during the deglaciation. By 18-17 ka, the SIS (light grey) had retreated and exposed the seas. Modified from Larsen et al. 2009.

The end of the LGM saw the beginning of the Baltic Ice Lake at 16 ka BP (Zillén et al. 2008). As the great ice sheets melted the most probable drainage areas for the glacial meltwater were the Öresund strait and lower valleys in Denmark (Andrén et al. 2011). As isostatic uplift in these areas was more rapid than eustatic sea level rise it resulted in altitudinal differences between the ocean and the Baltic Ice Lake. By 14 ka, the Kattegat-Skagerrak area resembled a fjord, with the ice front to the north and land areas to the south (Gyllencreutz et al. 2006).

1.4 Stable isotopes

Variations during the deglaciation and development of Kattegat to its present condition can be observed in the paleorecord using proxies such as oxygen and carbon isotopes. In fact, much of the climate reconstructions that have been done in the Baltic Sea, Kattegat and Skagerrak were possible due to the presence of oxygen and carbon in the water and fossil organisms that incorporate it into their shells.

Isotopes are variants of an element that carry different numbers of neutrons in the atomic nucleus, giving them different masses, while still retaining their characteristic chemical properties. There are two variations of oxygen used in paleoceanography, ^{16}O and ^{18}O. All oxygen contains 8 protons, but vary in the number of neutrons, making them lighter (^{16}O) or heavier (^{18}O). In some cases, such as in carbon, there can be both stable (^{12}C and ^{13}C) and radioactive (^{14}C) isotopes, the latter being used for radiocarbon dating rather than as a paleoenvironment proxy (Ravelo & Hillaire-Marcel 2007).

Lighter oxygen and carbon isotopes are the more commonly occurring on earth while the heavier ones are rarer. ^{16}O comprises 99.63% of all oxygen on Earth and ^{18}O comprises 0.1995%, while ^{12}C and ^{13}C make up 98.89% and 1.11%, respectively (Faure 1986). During natural processes such as evaporation, condensation, melting, crystallisation and diffusion, isotopes are separated due to their differences in mass as well as the temperature during the process, leading to variations in isotope ratios in e.g. seawater, ice and carbonate organisms (Allaby & Allaby 1999). It is thus the relationship between heavy and light isotopes that is essential in providing information about past environments when traced in e.g. marine shells.

To make small differences in the proportion of stable isotopes easier to interpret, values of isotopic measurements are expressed using a so-called "delta notation", defined as the difference in isotope ratio to a standard (Ravelo & Hillaire-Marcel 2007). The ratio (R) between heavy and light isotopes ($R = {}^{18}O/{}^{16}O$ for oxygen and $R={}^{13}C/{}^{12}C$ for carbon) in a sample is normalized to a known standard (Vienna Peedee Belemnite, VPDB, for carbonates and other rocks) and expressed

as a δ-value in ‰, as shown in the following equation (Katz et al. 2010):

$$\delta_{sample} = [(R_{sample} - R_{standard}) / R_{standard})] \times 1000\ ‰$$

Oxygen and carbon isotope ratios give values as $\delta^{18}O$ and $\delta^{13}C$, respectively. A positive δ-value means that the analysed sample has a higher proportion of heavy isotopes than the standard, while negative values mean the opposite. Accordingly, a δ-value of 0 shows that the sample and the standard (e.g. VPDB) have the same proportion of heavy and light isotopes (Ravelo & Hillaire-Marcel 2007).

1.4.1 Oxygen isotopes

Oxygen isotopic ratios in marine carbonates are often used as a proxy for temperature and salinity, since there are no instrumental measurements of these in the geologic past. As they grow, organisms such as foraminifera incorporate oxygen into their carbonate shells from the surrounding waters. By analysing the $^{18}O/^{16}O$ ratios in their shells ($\delta^{18}O_c$), it is therefore possible to calculate the oxygen isotope ratios of the water ($\delta^{18}O_w$) in which they lived, and in turn infer the environmental conditions. How organisms incorporate oxygen isotopes into their shells depend on two main factors:

1. The isotopic relationship of the surrounding waters ($\delta^{18}O_w$) during their lifetime,

2. The temperature in the water where they form.

The oxygen isotope ratio in water depends on several factors and changes depending on location as well as whether it is a glacial or interglacial period. ^{18}O is not as easily evaporated as ^{16}O since heavier isotopes require more energy to evaporate. As a consequence, water vapour has a more negative $\delta^{18}O$ value (less ^{18}O than the standard) than the ocean from which it is evaporated. Heavier isotopes also precipitate more readily, leading to clouds becoming more and more ^{18}O depleted the further inland or away from the equator they travel. Precipitation in continental settings or high latitudes thus often has very low $\delta^{18}O$ values, so that glacier ice can range from -35‰ to -50‰. The large amounts of light oxygen trapped in ice leaves the oceans with a comparatively high amount of ^{18}O, which in turn affects the $\delta^{18}O$ of the carbonates living in these waters. With this method, glacials and interglacials can be identified, as interglacial ocean water will have $\delta^{18}O$ values close to 0‰ while oceans during glacial ages have positive $\delta^{18}O$ values (around +1‰).

The global ice volume effect on seawater $\delta^{18}O$ is an essential aspect that must be factored into paleotemperature equations. Table 1 (Fairbanks et al. 1992; Bemis et al. 2002) shows the effect on $\delta^{18}O$ of seawater globally during the deglaciation, due to the shrinking ice caps. This change is not an effect of altered salinity or temperature in a specific basin and should not be mistaken as local paleoenvironmental variations. The local effects on a basin's $\delta^{18}O$ changes are freshwater input (from meltwater or rivers), evaporation/precipitation patterns and changes in advection or upwelling of water with different $\delta^{18}O$ (Ravelo & Hillaire-Marcel 2007).

The relationship between water $\delta^{18}O_w$ and carbonate $\delta^{18}O_c$ is controlled by processes known as fractionation. Shells formed in colder water typically have more positive $\delta^{18}O$ values than those formed in warmer water, such that a 1°C increase in temperature results in a $\delta^{18}O_c$ decrease of 0.25‰ (less ^{18}O) (Katz et al. 2010). The relationship can be expressed by the following paleotemperature equation established by Epstein et al. (1953):

$$T\ (°C) = 16.5 - 4.3(\delta_C - \delta_W) + 0.14(\delta_C - \delta_W)^2$$

δ_c is the $\delta^{18}O_c$ in a carbonate sample and δ_w is the $\delta^{18}O_w$ in seawater. The equation has later been modified by Craig (1965), O'Neil et al. (1969), Shackleton (1974) and Bemis et al. (2002) among others.

The carbonate $\delta^{18}O$ can in many cases also be influences by the salinity in the seawater, especially in the Baltic Sea basin during the deglaciation since its salinity fluctuations have been more significant than its temperature. In fact, salt does not affect $\delta^{18}O$ directly, but can be inferred as a result of changes in the hydrological cycle, evaporation, precipitation and moisture transport. Summarising, more positive $\delta^{18}O$ values indicate larger global ice volume or colder and more saline waters while more negative $\delta^{18}O$ values indicate smaller global ice volume as well as warmer and fresher waters (Katz et al. 2010).

1.4.2 Carbon isotopes

In seawater, $\delta^{13}C$ is primarily related to the dissolved inorganic carbon (DIC) present (Urey 1947). On a global scale the change in carbon isotope composition of DIC ($\delta^{13}C_{DIC}$) in the oceans depends on how much carbon is released from the lithosphere (by hydrothermal or volcanic outgassing and chemical weathering of continental rocks), how much carbon is removed from the oceans (by deposition in marine

Table 1. Global change in $\delta^{18}O_w$ due to the volume of ice locked in ice caps, from 19 – 13 ka. Modified from Bemis et al. (2002).

Age (ka)	Ice volume effect, $\Delta\delta^{18}O_w$ (‰)
13.0	0.56
14.0	0.66
15.0	0.84
16.0	0.87
17.0	0.91
18.0	0.93
19.0	1.00

sediments) and the growth of terrestrial biosphere (causing $\delta^{13}C_{DIC}$ to increase). Locally, $\delta^{13}C_{DIC}$ reflects circulation patterns (such as advection, upwelling and waters with different $\delta^{13}C_{DIC}$ signatures reaching the site), photosynthesis (causing an increase in local $\delta^{13}C_{DIC}$) and respiration (causing a decrease in $\delta^{13}C_{DIC}$) (Ravelo & Hillaire-Marcel 2007).

Primary producers such as plankton and plants prefer to incorporate the lighter carbon isotope ^{12}C, and consequently have a lower $\delta^{13}C$ signature (as low as -25‰ for land plants but higher values for marine plants; Park & Epstein 1960). This process of discriminating against heavy carbon isotopes is called biological fractionation and affects the seawater $\delta^{13}C_w$ so that more primary producers incorporating ^{12}C from their surroundings leads to higher relative levels of ^{13}C in the water. In turn, biocalcifying organisms in these waters thereby reflect the high $\delta^{13}C$ values in their shells (Katz et al. 2010).

When organic matter sinks and collects at the bottom, nutrients and CO_2 with low $\delta^{13}C$ signals are released. As a result, the $\delta^{13}C_{DIC}$ of the water mass becomes more negative with longer residence time (or the further the water mass flows from its source). Besides being a sign of residence time, low bottom water $\delta^{13}C_{DIC}$ values typically indicate a high content of organic matter (Filipsson & Nordberg 2010). In these scenarios, oxygen deficiency is common because oxygen is consumed by processes of degradation of organic matter. Strong stratification can further promote low oxygen conditions as deeper water is not exposed to the atmosphere's oxygen when a basin is stagnant (Katz et al. 2010). Because different oceans have their own characteristic $\delta^{13}C$ signature, temperature, salinity and nutrient content, the $\delta^{13}C$ variation in a basin can represent changes in circulation patterns and influences of waters from other locations, thereby often revealing salinity changes, which in some cases are related to $\delta^{13}C$ fluctuations (Wright et al. 1991).

1.5 Foraminifera

Changes in water $\delta^{18}O$ and $\delta^{13}C$ cannot be directly measured in the past, but can be calculated using calcifying organisms. Foraminifera are vastly used for this purpose because of their ability to form tests (shells) from elements in the seas they inhabit. These small (usually <1 mm) unicellular protists are among the most studied calcareous microfossils. Most species have tests composed of calcium carbonate ($CaCO_3$), although some have agglutinated or only organic shells. Marine foraminifera are either planktic (surface-dwelling) or benthic (usually living on or in the upper centimetres of the sea floor).

As the foraminifera grow, mineral matter from their surroundings is precipitated into their tests, in a mineralisation process not fully understood (Boersma et al. 1998). The geochemical signature of their tests, however, relates to the chemical and isotopic composition of the waters in which they lived and grew (Duplessy et al. 1984), and it is their ability to incorporate elements from the water in their habitat that make them excellent paleoenvironmental indicators of climatic conditions in the time and place where they lived. Metabolism, habitat preferences and isotopic fractionation vary depending on the species and can give different results even if they are found in the same location and depth. This can, to a large extent, be avoided by selecting a single species and a limited size range to perform isotope analyses on. In the core presented in this thesis, the most abundant species is *Elphidium excavatum* f. *clavatum*, a benthic foraminifer found to inhabit all types of sediments (Figure 3). *E. excavatum* often dominate foraminiferal assemblages in the most extreme conditions, such as environments with low salinities, low oxygen and high turbidity, although Hald et al. (1994) found that they prefer temperatures between 1°C and -1.8°C and salinities around 33. They are most typically found in arctic settings with cold and turbid water close to retreating glaciers (Hald & Korsun 1997).

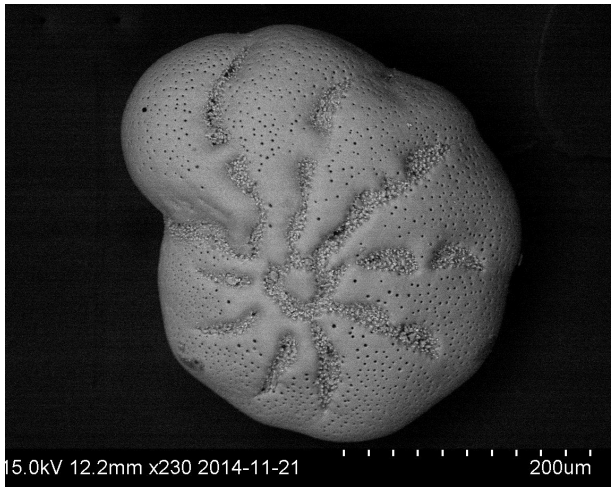

Fig. 3. SEM image of a foraminifera from Kattegat, species *Elphidium excavatum*. Photo: N.B. Quintana Krupinski, 2015.

2 Methods

2.1 Sample collection

This thesis presents a foraminifera isotope record from core M0060A, Anholt island, Kattegat (56°37.21′N, 11°40.24′E). The core was collected during IODP Expedition 347 on the ship Greatship Manisha between the 23rd and 29th of September 2013 at a water depth of 31.2 m. The coring reached a total depth of 232.5 m. For the upper ~83 m piston coring was used and the recovery was >90%. On greater depths, however, combinations of piston coring, non-rotating core barrel, extended nose coring, open holing, hammer sampling and push coring were used, but recovery and core quality were limited. The section used in this thesis is 82.50 – 9.62 mbsf and consists of the following lithology units, from deeper to shallower (Figure 4):

- Unit IV, 82.50 – 79.52 mbsf: gray interbedded sand, silt and clay.
- Unit III (a, b and c), 79.52 – 23.84 mbsf: gray parallel laminated silty clay (or clay and silt for unit IIIa).
- Unit II, 23.84 – 9.62 mbsf: dark greenish gray interlaminated sandy clayey silt and fine-medium sand (Andrén et al. 2015).

The depth range presented here (82.50 – 9.62 mbsf) contains the core's best, longest record of non-reworked foraminifera and spans the time period of the last deglaciation in northern Europe.

2.2 Sample preparation

The core was sampled at a depth resolution of 25 – 100 cm as follows:

- 9.62 – 20.97 mbsf: 1 sample/m
- 21.38 – 72.80 mbsf: 3 samples/m
- 73.03 – 82.50 mbsf: 4 samples/m

Samples containing 20 cm^3 each were put in small plastic bags and freeze-dried. The dry samples of sediment were weighed and a small fraction (~1 g) of sediment was removed to store as an archive. The non-archive portion of each sample was soaked with a laboratory detergent ($Na_4P_2O_7$) dissolved in DI-water (deionised water) and put on a shaker table for a few hours or overnight. The samples were then washed over a 63µm sieve with DI-water, rinsed with ethanol to prevent potential isotope fractionation effects of water evaporation, and left to air dry on filter paper, after which the dry >63µm sediment was weighed and stored in glass vials. The ratio of the >63µm size fraction to the dry bulk sediment weight was used as a measure of weight percent coarse fraction.

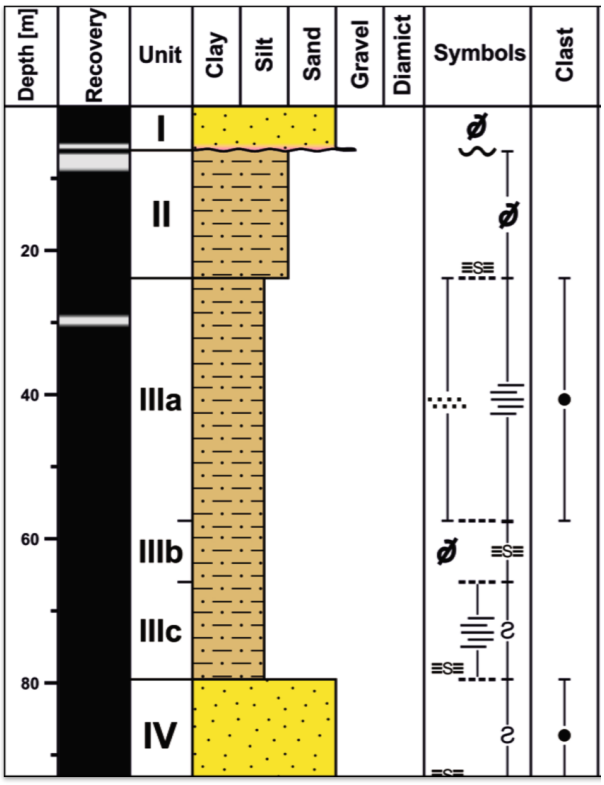

Fig. 4. Lithostratigraphy of the upper ~85m of site M0060A, divided into units. This part of the core had a recovery of >90%. Modified from Andrén et al. 2015.

2.3 Foraminifera picking

Prior to picking of foraminifera, the samples were put through sieves of 500µm, 355µm, 250µm, 125µm and in some cases 100µm. Each fraction was inspected under a light microscope for macrofossils and foraminifera. The latter were picked out and placed on slides according to size. Macrofossils were also picked out for ^{14}C dating and placed on slides indiscriminately of size or kind. Redeposited pre-Quaternary foraminifera (generally Cretaceous) were not picked when identifiable as such.

All the laboratory work (sample preparation, foraminifera picking and weighing) was carried out by myself within my master's student project in the Department of Geology at Lund University between November 2014 and June 2015 under the supervision of Nadine Quintana Krupinski and Helena Filipsson. The lab equipment was provided by the Dept. of Geology.

2.4 Stable isotope analysis

20-60µg (7 – 15 individuals) of single-species benthic foraminifera (*Elphidium excavatum,* f *clavatum)* were selected from a restricted size range (125-250µm) for isotopic analysis. The samples were sent to the stable isotope lab at the Alfred Wegner Institute, Bremerhafen, Germany, for oxygen and carbon isotope analysis. Analytical precision is based on replicate measurements of in-house carbonate standard Solnhoffen limestone (SHKBR3). Reproducibility of SHKBR3 is ± 0.040‰ for $\delta^{18}O_{CaCO3}$ and ± 0.041‰ for $d^{13}C_{CaCO3}$ (1σ; n= 39), meaning that any variations in foraminifera stable isotope results smaller than this cannot be distinguished from the instrumental error.

2.5 Age model

An age model was provided by Aarno Kotilainen, Outi Hyttinen and Nadine Quintana Krupinski, based on 15 ^{14}C samples dated at Radiocarbon Laboratories in Poznan and Zurich. Out of the 15 samples dated and used for the age model, 10 are marine mollusc shells and 5 are benthic foraminifera. Linear interpolation was used and an age model graph was made by Kotilainen and Hyttinen (Appendix 1).

3 Results

3.1 Stable oxygen and carbon isotopes

Of the 201 samples washed and picked, 107 foram-

inifera samples were analysed for stable oxygen and carbon isotopes (Appendix 2). An additional 21 samples were analysed in duplicate, and duplicates were averaged together before further data processing. 94 of the washed sediment samples did not yield stable isotope results because A) insufficient foraminifera were present (20µg of *Elphidium excavatum clavatum* in the 125-250µm size fraction were required), and B) a small number of analysed samples (4-6) were discarded due to errors in the laboratory.

The average age resolution of the isotope record is ~36 years, though the sample resolution is as high as 9 years in the interval 82.5 – 80.03 mbsf, and as low as 138 years in 18.68 – 9.62 mbsf. The results are subdivided into 5 stages based on changes in the trends of the $\delta^{18}O$ and $\delta^{13}C$ values.

3.1.1 $\delta^{18}O$

The mean value of $\delta^{18}O$ for the whole record is 0.9‰, with a maximum of 3.3‰ at 81.51 mbsf, and a minimum of -0.8‰ at 21.38 mbsf. There is a mean decrease of 2.3‰ from the deepest to the shallowest portion of the core (calculated from the average of six values at each end) (Figure 5).

Stage A: 82.50 - 73.80 mbsf: This stage has the most positive values of the entire core (maximum 3.3‰ at 81.51 mbsf, minimum 0.8‰ at 79.12 mbsf). The decline from the beginning to the end of A (82.50 – 73.80 mbsf) is 1.2‰ and the mean value for stage is 1.8‰, almost 1‰ higher than the entire average. $\delta^{18}O$ declines rapidly in this stage (0.3‰ per 1 m).

Stage B: 73.80 – 51.63 mbsf: This stage shows large, rapid $\delta^{18}O$ oscillations between a maximum value of 1.9‰ at 61.44 mbsf and a minimum of 0.2‰ at 55.67 mbsf. The mean value of area B is 1.0‰, which is more negative than A. $\delta^{18}O$ declines more gradually in this stage (0.08‰ per 1 meter).

Stage C: 51.63 – 32.37 mbsf: In stage C, $\delta^{18}O$ declines by 1.0‰ between 48.75 and 32.37 mbsf. The maximum value is 1.5‰ at 42.33 mbsf and the minimum is -0.1‰ at 32.37 mbsf,. The mean value is 0.7‰ for area C; more negative than both stages A and B.

Stage D: 32.37 – 21.38 mbsf: In stage D, $\delta^{18}O$ declines by 0.9 ‰. The mean value is -0.1‰, which makes stage D the most negative part of the core. The maximum value is 0.7‰ at 26.75 mbsf, and the minimum is -0.8‰ at 21.38 mbsf, the latter being the lowest value in stage D as well as the entire core.

Stage E: 20.97 – 9.62 mbsf: Stage E shows large $\delta^{18}O$ oscillations, and a $\delta^{18}O$ decline of 0.4‰. It has a maximum value of 0.9‰ at 15.63 mbsf and minimum of -0.5‰ at 9.62 mbsf. E's mean value is 0.2‰, which is the lowest after stage D.

3.1.2 $\delta^{13}C$

Stages A – D show large oscillations around a stable mean $\delta^{13}C$ value (-2.8‰). Stage E, however, shows a trend of increasing $\delta^{13}C$ values. The mean value of $\delta^{13}C$ for the whole record is -2.8‰, with a maximum of -1.5‰ at 16.63 mbsf, and a minimum of -4.4‰ at 67.53 mbsf. There is a mean increase of 0.7‰ from the deepest to the shallowest parts of the core (calculated from the average of six values at each end) (Figure 6).

Stage A: 82.50 – 73.80 mbsf: This stage shows oscillating values with a maximum of -2.2‰ at 77.90 mbsf and a minimum of -3.6‰ at 79.12 mbsf. The mean value of stage A is -2.9‰.

Stage B: 73.80 – 51.63 mbsf: This portion has a maximum value of -2.2‰ at 61.44 mbsf and a minimum of -4.4‰ at 67.53 mbsf, giving an increase of 2.2‰ over 6.09 m. The mean value is -3.0‰, which is more negative than stage A.

Stage C: 51.63 – 32.37 mbsf: This stage has less oscillation than the aforementioned stages. The maximum value is -2.5‰ at 45.47 mbsf and the minimum is -3.5‰ at 48.25 mbsf, giving an increase of 1.0‰ over 2.78 m. The mean value is -2.8‰, which is more positive than stages A and B.

Stage D: 32.37 – 21.38 mbsf: The maximum value is -2.6‰ at 28.86 mbsf, and the minimum is -3.7‰ at 21.95 mbsf. This gives a decrease of 1.1‰ within 6.91 m. The mean value is -3.0‰, which makes D the most negative stage of the core on average, even though stage B contains several values more negative than those found in D.

Stage E: 21.38 – 9.62 mbsf: Stage E is the core's shallowest portion. It has a maximum value of -1.5‰ at 16.63 mbsf and minimum of -2.7‰ at 19.57 mbsf, an increase of 1.1‰ within 2.9 m. The mean value of E is -2.2‰, which makes it the most positive portion. It contains several of the core's highest values, with no point below the entire core's mean value. In fact, all of the 9 shallowest data points exceed -2.2‰. Higher values only occur twice in any other interval, namely at 61.44 mbsf and at 77.90 mbsf.

3.1.3 Correlation of $\delta^{18}O$ and $\delta^{13}C$

The correlation (r^2) between $\delta^{18}O$ and $\delta^{13}C$ is close to 0 for all values (r^2=0.0012. The stages with the highest correlation between $\delta^{18}O$ and $\delta^{13}C$ are A (r^2=0.244) and E (r^2=0.260), while B, C and D have r^2 values of 0.088, 0.188 and 0.040 respectively.

3.2 Grain size (weight percent coarse fraction)

The weight ratio of sediments >63µm to total bulk sediment dry weight (wt. % coarse) is used to quantify the percentage of coarse sediment, which includes gravel, sand, mollusc shells, foraminifera, etc. In the upper (27.86 – 9.62 mbsf; lithostratigraphic units II and upper IIIa) and lower (82.5 – 79.28 mbsf, lower unit IIIc and upper IV) intervals of this record (Figure 4)(Andrén et al., 2015) coarse sediment composes >10% of the total sediment by mass (Figure 7), and between 23.64 and 9.62 mbsf, coarse sediment is generally 20-60%.

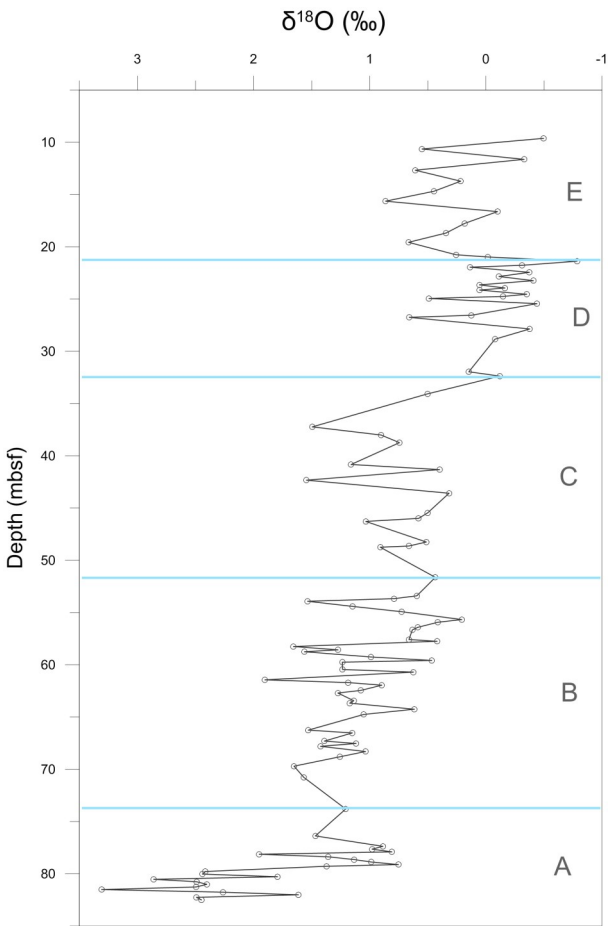

Fig. 5. Graph of $\delta^{18}O$ values plotted against depth. The record has been divided into five different stages, according to apparent trends. Note that the $\delta^{18}O$ values are plotted in descending order from left to right.

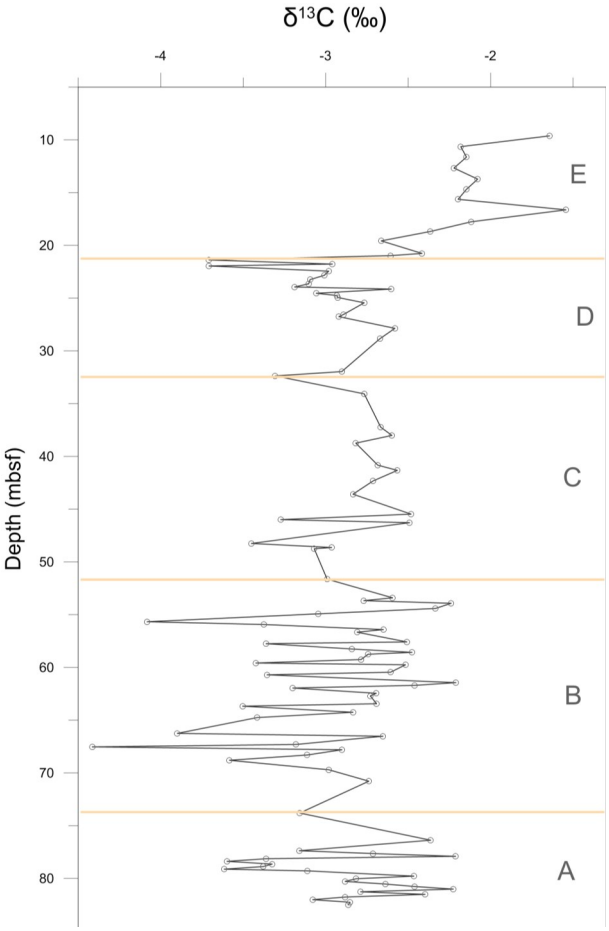

Fig. 6. Graph of $\delta^{13}C$ values plotted against depth. The record has been divided into five different stages, according to apparent trends.

Conversely, the interval between 79.12 and 28.84 mbsf (Unit III) contains <6% coarse sediment, and generally <3%, in agreement with the description of this interval as primarily silt and clay (Andrén et al., 2015). Peaks in wt. % coarse in this interval (Unit III) represent a combination of increased sand proportion and increased foraminiferal content. Most of the samples with wt. % coarse <1% are barren of foraminifera with some exceptions, such as 70.78 mbsf with only 0.18% coarse grains, most of which consists of foraminifera; or 64.75 mbsf, which has only 0.93% coarse sediment but abundant foraminifera. In 80.01 mbsf there was a larger clast present (~1 cm) weighing 2.8g, and in 74.80 mbsf much of the sediment was >355µm and some >500µm.

3.3 Mean shell weight

Because the foraminifera used for analysis and weighed are from a restricted size range (125-250µm), the mean shell weight per foraminifera indicates variations in shell thickness. A five-point smoothing line is helpful to show trends in shell weight more clearly (Figure 8). Background shell weight values from 82.5 – 24.54 mbsf are generally ~2-4µg, but several short peaks in mean shell weight (5-8µg) occur at 78.38, 67.80, 64.75, 62.7 and 34.07 mbsf. Between 24.54 and 23.24 mbsf, shell weight rises from 2.6 to 6.7µg, and from 23.24 – 9.62 mbsf, shell weight values show a long decline from ~7µg to ~2µg.

4 Discussion

The samples used in this thesis represent the deglaciation of the late Weichselian in southwest Scandinavia (Lagerlund & Houmark-Nielsen 1993). According to the age model for site M0060A (Appendix 1; Kotilainen & Hyttinen, unpublished) the depths 82.50 – 9.62 mbsf correspond to an age range of 18.1 – 14.3 ka BP, making it an important time in the history of Kattegat since it could potentially reveal interesting events of the most recent deglaciation. The stable isotope results generated from benthic foraminifera analyses reveal conditions on the seafloor during this time interval, such as changes in temperature and salinity ($\delta^{18}O$) as well as ventilation, productivity and oxygenation ($\delta^{13}C$).

4.1 Stable oxygen and carbon isotopes

4.1.1 $\delta^{18}O$

Anholt during the deglaciation is likely to have had fluctuations in both sea bottom temperature and salinity. When the Scandinavian Ice Sheet (SIS) melted, however, it discharged large amounts of fresh water into the surrounding seas, thus possibly influencing salinity of surface and bottom waters to a larger extent than temperature. As Kattegat is positioned between the brackish Baltic Sea and the saline Skagerrak and North Atlantic Sea, it is particularly susceptible to salinity changes.

The $\delta^{18}O$ results previously presented in figure 5 have also been plotted against time, with a 3-point smoothing line (Figure 9) to make trends more visible. More negative $\delta^{18}O$ values usually represent water that is fresher, warmer or both, while more positive values represent colder or more saline waters. The oldest stage starts off very positive but displays a 1.5‰ decrease over approximately two centuries. This suggests a rapid freshening in the beginning of the record, likely as a result of a large release of glacial meltwater. The subsequent stages show a slower $\delta^{18}O$ decrease (2.4‰ over ~1.9 ka), reaching a minimum at ~15.7 ka, which suggest that most of the record reflects further, more gradual freshening of the waters in Kattegat until ~15.7 ka. In the youngest stage (15.7 – 14.3 ka), the $\delta^{18}O$ trend changes and values quickly increase, which suggests that the water mass became more saline after the long period of freshening, though not reaching values as high as before ~16.6 ka. The relative changes described above give information about the trends and possible events that could have taken place during this time.

As we lack instrumental temperature and salinity data concerning paleoenvironmental conditions, we have to make certain assumptions in order to attempt to obtain more specific estimates from our data sets. For example, when analysing $\delta^{18}O$ we could start by assuming a constant water temperature as well as constant fractionation to be able to calculate the maximum change in salinity that could have occurred within the span of our core. Although our estimated results are less than perfect it at least gives us an amplitude of values that we may consider, and allows us to describe possible paleoenvironmental scenarios for the Kattegat during the most recent deglaciation.

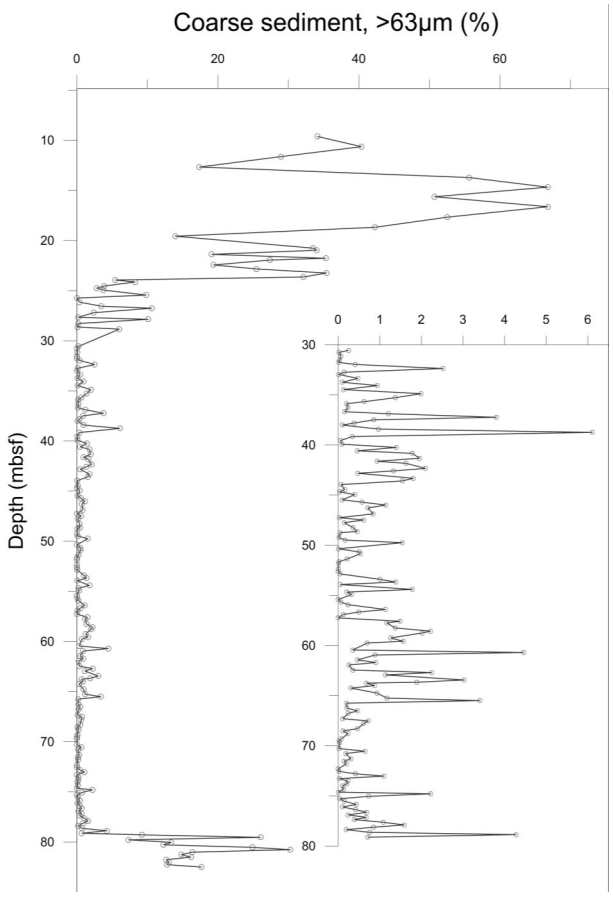

Fig. 7. Weight percent coarse sediment plotted against depth, with an inset showing the values close to 0% more clearly. Samples in the deepest and shallowest portions of the core have values 10—70%, while most of the record remains between 0 and <7%.

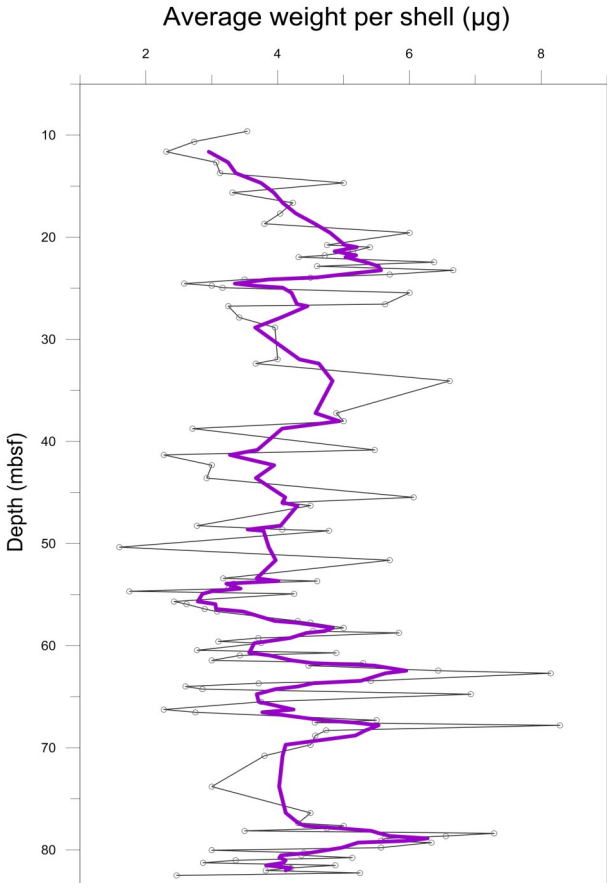

Fig. 8. Average weight per foraminifera shell plotted against depth. A 5-point smoothing line has been applied to facilitate discernment of trends, such as the shallow portion which shows a decrease in shell weight.

4.1.2 Salinity reconstruction

The first empirical temperature-$\delta^{18}O$ relationship was produced in 1947 by Harold Urey (Urey 1947). After that, several other equations have been developed by Epstein et al. (1953), Shackleton (1974), O'Neil et al. (1969) and Bemis et al. (1998), among others. Calculations differ depending on site, temperature range, source (i.e. what material or organism is used), and in case of foraminifera it can even make a difference how many chambers the shell has (Bemis et al. 1998), but they stem from the same basis:

$$T(°C) = a + b\,(\delta_c - \delta_w) + c(\delta_c - \delta_w)^2$$

where δ_c is the $\delta^{18}O$ of calcite and δ_w is the $\delta^{18}O$ of water. The letters a, b and c are constants but differ depending on the study. The equation by Epstein et al. (1953) set a=16.5, b=-4.3 and c=0.14. This was done on molluscs, however and could be different from values derived from foraminifera. Shackleton (1974) modified the equation from O'Neil et al. (1969) using inorganic material and calibrated it with the benthic foraminifera genus *Uvigerina*.

Using a species-specific equation gives a higher chance of getting a reliable result, as opposed to applying generic equations or equations developed for another species, since this can over- or underestimate the calcification temperatures for the species at hand (Bemis et al. 2002). I use a linear equation in the format shown here, instead of the quadratic equation shown above:

$$T(°C) = a + b\,(\delta_c - \delta_w)$$

Quadratic equations have been developed because the isotopic fractionation factor between a mineral and water is predicted to vary with a logarithmic scale in very high and very low temperatures, but this is not necessary to take into consideration when working with moderate temperature ranges (defined differently in the various studies) (Bemis et al. 1998). Using linear equations at very low temperatures can nevertheless be misleading, and should therefore be approached with the sufficient knowledge of its impact on the results. From our *Elphidium excavatum clavatum* oxygen isotope results we know δ_c ($\delta^{18}O_c$) for each depth, but paleotemperature (T) and $\delta^{18}O$ of water where the forams calcified (δ_w or $\delta^{18}O_w$) are unknown, so to solve for seawater $\delta^{18}O$ and salinity we must assume a

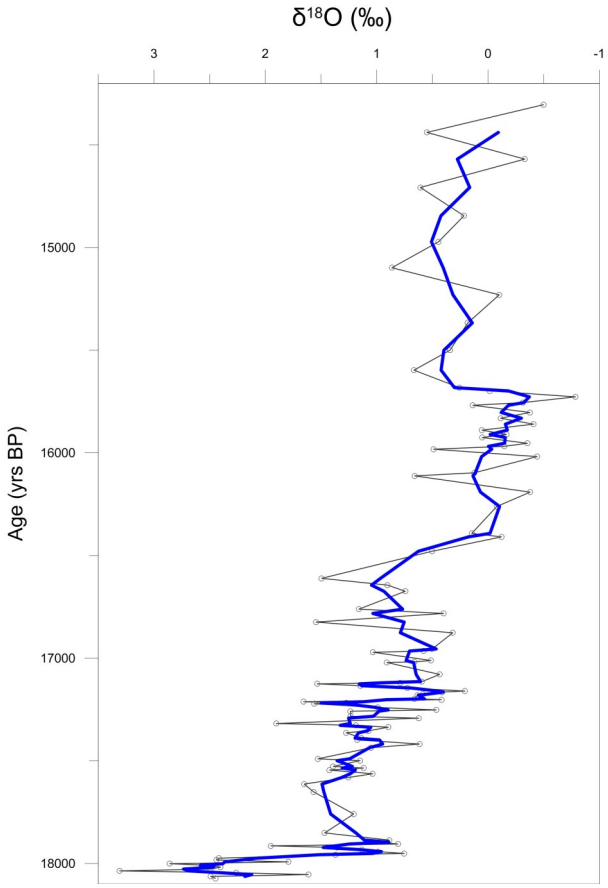

Fig. 9. Graph of $\delta^{18}O$ values plotted against age with a 3-points smoothing line. The values suggest rapidly decreasing salinity in the beginning of the record, followed by a more gradual decrease until 15.7 ka where it increases.

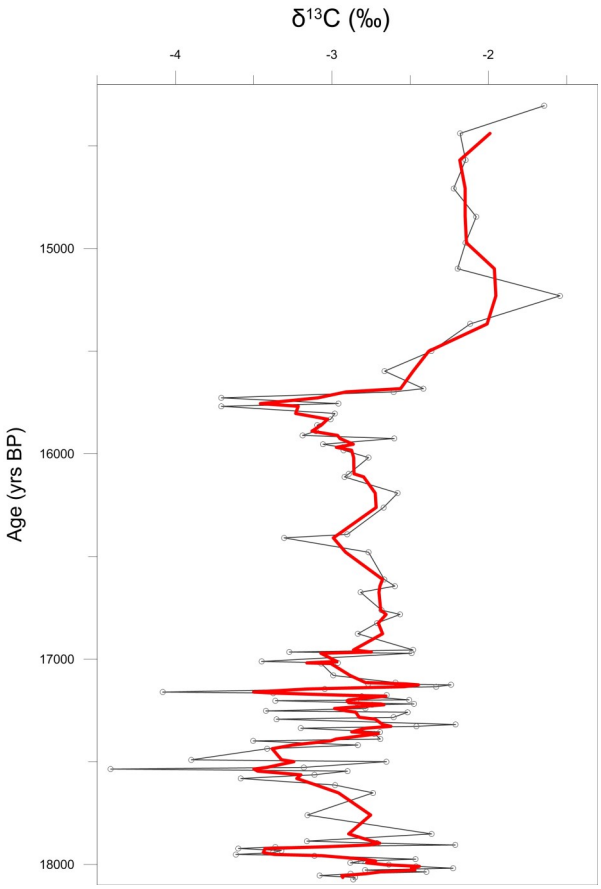

Fig. 10. Graph of $\delta^{13}C$ values plotted against time with a 3-point smoothing line. The values oscillate from 18—15.7 ka, where they increase and remain higher for the rest of the record.

water temperature.

By studying modern sites that have characteristics of deglacial environments and have the foraminifera *Elphidium excavatum*, we can make reasonable temperature estimations for the Kattegat 18 – 14 ka BP. Hald & Korsun (1997) present bottom water temperatures and salinities in several Svalbard fjords (European Arctic), together with benthic foraminifera assemblages (including *Elphidium excavatum clavatum*), which range between -1.5°C and +3°C. Bottom waters off North Iceland display temperatures of 0 – 3° C (Knudsen et al. 2012), which gives us a limited range of possible values to consider. Waters with salinities of 35 freeze at approximately -2°C (depending on pressure), but since present Anholt bottom salinities are 33.5 – 34.5, and were presumably lower during the deglaciation, such low bottom temperatures are less likely. Instead, a temperature range between -1°C and +1°C was proposed by Karen Luise Knudsen (personal email contact, October 2015). However, such low temperatures yield salinities as low as 10, which is unrealistic.

Elphidium excavatum is found in the present Skagerrak and Kattegat in salinities between 15 and 31. At lower salinities there is a small probability of shell preservation, so due to the generally good condition of shells in our record it is likely that salinities were mostly within this range (Alve & Murray 1999). A temperature of 3°C is assumed, as it fits with the aforementioned studies. $\delta^{18}O_w$ has been calculated from each of the following three equations using a constant temperature of 3°C (Figure 11):

Equation 1. Epstein et al. (1953): They used molluscs for calibration and the linear equation yields results closest to the quadratic form in the temperature range 9 – 24°C. $T(°C) = 16.6 + 4.3 (\delta_c - \delta_w)$.

Equation 2. Shackleton (1974): He modified a previous equation by O'Neil et al. (1969) based on inorganic carbon, and calibrated it for the benthic foraminifera genus *Uvigerina*, recommending it for temperatures 0 – 16.9°C. $T(°C) = 16.9 + 4.0 (\delta_c - \delta_w)$.

Equation 3. Bemis et al. (2002): Also calibrated the equation to *Uvigerina* from the Southern California Bight, in the temperature range 3.9 – 6.8°C. $T(°C) = 21.6 + 5.5 (\delta_c - \delta_w)$.

In order to convert δ_w ($\delta^{18}O_w$) to salinity, the equation "Mixing line for the Skagerrak-Baltic Sea region" developed by Filipsson et al. (2015, unpublished) for present day conditions is used:

$$\delta^{18}O_w = 0.25 \times S - 8.61$$

where S is salinity. The ice volume effect (see Table 1) for each sample's calculated $\delta^{18}O_w$ is subtracted according to its corresponding age before calculating salinity (the values have been interpolated and applied to all ages corresponding to the samples in this thesis). All salinity calculations henceforth will be corrected for ice volume effect.

Since Epstein's equation is calibrated for molluscs and recommends a temperature of 9 – 24°C, there is a risk of getting too large of an error, and thus a *Uvigerina*-calibrated one seems more appropriate for *E. excavatum* based oxygen isotope values. Shackleton is preferred over Bemis since the latter experiments were carried out in a California basin, an area very different from the setting presented (Figure 12).

Because the change in salinity derived from the $\delta^{18}O$ record is identical regardless of the temperature applied (if a constant temperature is assumed), we can calculate a decline in salinity of 16 units between 18 and 15.7 ka. We can regard this as a maximum salinity change, since changes in temperature likely account for a portion of the $\delta^{18}O_c$ signal.

A more realistic assumption is that temperature changed during the period 18 – 14.3 ka. While temperatures may have fluctuated in this time period (e.g during the interstadial Bölling-Alleröd), lacking independent temperature information, we can instead test a scenario in which temperature increased linearly from 0°C at 18 ka to 4°C at 14.3 ka (Figure 13). Though a constant linear temperature rise is an oversimplification and only one of several possible scenarios, this

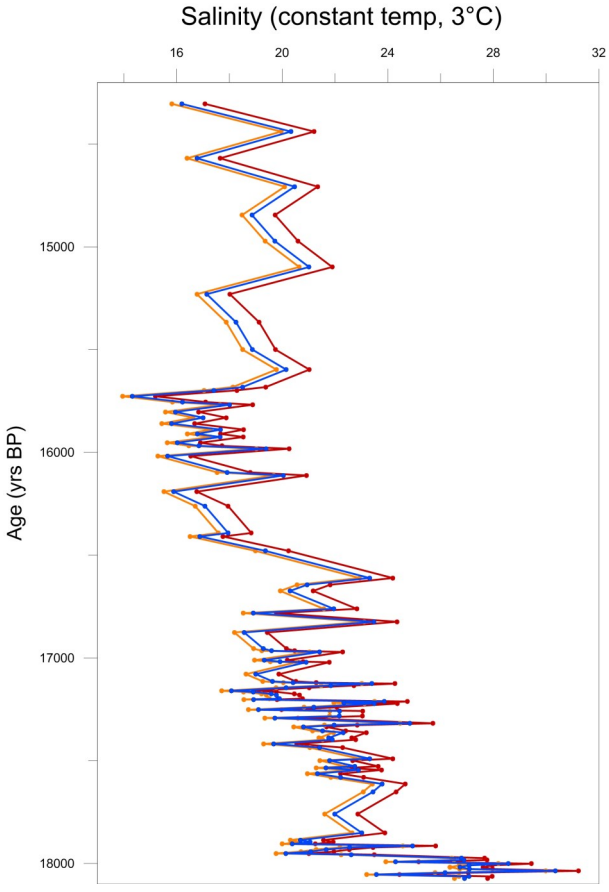

Fig. 11. Salinity values calculated with Filipsson's "Mixing line for the Skagerrak-Baltic Sea region", using $\delta^{18}O_w$ values calculated with the equations by Epstein (red), Shackleton (orange) and Bemis (blue), with an assumed constant temperature of 3°C. Bemis and Shackleton show very similar values while Epstein gives a higher salinity for the same temperature. Ice volume effect is applied to all values.

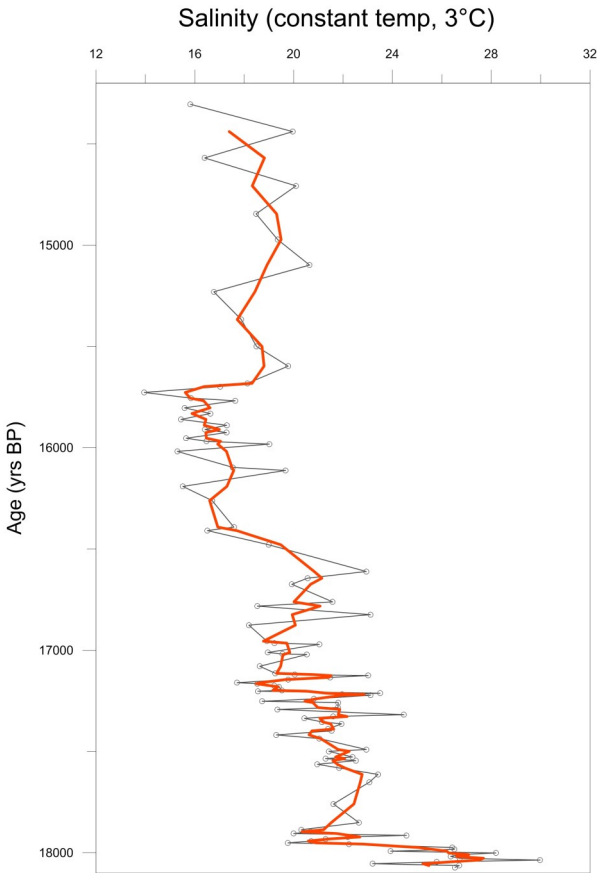

Fig. 12. Salinity values using Shackleton's equation with an assumed constant temperature of 3°C. A 3-point smoothing line has been applied for easier viewing but calculated values are reported. The maximum salinity is 30 at 18.1 ka BP, and the minimum is 14 at 15.7 ka BP, a difference of 16 units. When applying lower temperatures, the salinity values come out lower, such that a 1°C decrease gives a salinity decrease of 1, but the difference between the max and min is the same.

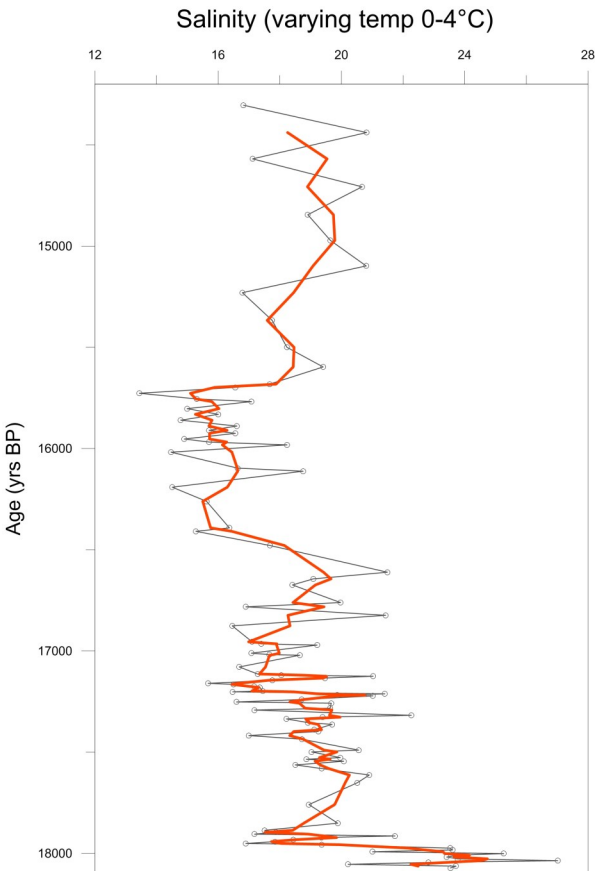

Fig. 13. Salinity values using Shackleton's equation with an assumed linear temperature increase from 0°C to 4°C from 18.1-14.3 ka. This scenario shows a smaller increase in salinity change from beginning to end compared to the constant temperature scenario, with salinities at ~18 ka lower, and salinities from ~15.6 ka higher than when using a single temperature throughout the time frame.

allows us to explore how salinity in this area could have changed with increasing temperature.

In this scenario of linearly increasing temperature, the difference between the maximum salinity (27 at 18 ka BP) and the minimum salinity (13 at 15.7 ka BP) is a decrease of 14 instead of 16 over the first ~2.3 ka, while the salinity increase from 15.7 to 14.3 ka is larger in the changing temperature scenario. In this scenario, during the first two centuries, bottom waters rapidly freshened by almost 10 units, then over the next 2 ka, freshening continued more gradually (6 units) until 15.7 ka. Between 15.7 and 14.3 ka, salinity increased by almost 8 units.

This salinity increase after 15.7 ka could represent a change in the in- and output of water in Kattegat. According to Knudsen et al. (1996) who studied the paleoenvironment in the Skagerrak-Kattegat basin during the deglaciation, an increase in $\delta^{18}O$ suggests an influence of higher salinity waters. When there is a large meltwater supply to the basin, the density difference between fresh surface and saline bottom waters leads to stratified conditions in the water column. Saline bottom waters from the North Sea or Atlantic flow in to the basin to compensate for this outflowing surface water. Accordingly, low $\delta^{18}O$ values can be a result of a reduced meltwater supply, leading to less stratification and in turn lower salinities at the seafloor due to increased mixing with the fresh surface waters. Consequently, high salinity of bottom water is a result of stronger stratification, and vice versa. During glacial periods colder stadials are characterised by ice growth and advance, while relatively warmer interstadials typically have ice retreat and therefore larger quantities of fresh water being discharged from the melting ice into the basin (Knudsen et al. 1996).

4.1.3 $\delta^{13}C$

The $\delta^{13}C$ values of foraminifera analysed for this thesis have very negative values (a mean of -2.8‰, ranging from -1.5 to - 4.4‰) compared to other studies in settings that are presumably similar. *Elphidium excavatum* in Skagerrak-Kattegat (15 – 8.6 ka) studied by Knudsen et al. (1996) had $\delta^{13}C$ values ranging from -1 to -3‰. Mackensen (2013) studied recent benthic

foraminifera (*Cibicidoides wuellerstorfi*) in the deep Arctic Ocean and found that the mean $\delta^{13}C$ was 1.22‰. A study by Filipsson et al. (2004) in western Swedish fjord sediments (Gullmar Fjord and Havstens Fjord) found $\delta^{13}C$ values in benthic foraminifera (*Stainforthia fusiformis*) between -1.2 and -2.6‰. It should be considered, however, that *Elphidium excavatum* is an infaunal species, which results in lower $\delta^{13}C$ values than epifaunal species at the same site (Mackensen et al. 2000). A study in the Barents and Kara Seas concluded that *E. excavatum* had the lowest $\delta^{13}C$ values of the nine species analysed, which suggests the deepest infaunal habitat (Hald et al. 1994).

As seen in figure 10, the $\delta^{13}C$ values are low but relatively stable in the early part of the core (18 – 15.7 ka), with an increase from 15.7 to 14.3 ka. This could suggest stagnant conditions due to strong salinity stratification during the earlier stage, followed by improved ventilation, more mixing and increased bottom water oxygen levels between 15.7 and 14.3 ka. Such a proposed change in ventilation could indirectly indicate a decrease in the amount of glacial meltwater flowing into the basin, since more freshwater input gives stronger stratification and less ventilation, owing to the density contrast between the shallow and deep water bodies.

The low values suggest an ice-proximal setting similar to a fjord, where the bottom water has a long residence time due to the limited mixing. The bottom water can remain stagnant until a storm or similar inflow event provokes waters to flush or mix, bringing in more oxygenated and saline water (Farmer & Freeland 1983), and is possibly what happened at 15.7 ka when $\delta^{13}C$ values increase. This could be a combination of a decrease in fresh water input as well as a larger inflow of seawater from the North Sea to Kattegat. Apart from larger seawater quantities, a sudden change in $\delta^{13}C$ values can also be attributed to a changed water origin, due to the varying $\delta^{13}C$ signals of different water masses.

Several authors note the importance of the period 18 – 15 ka in the history the deglaciation in Kattegat. According to Houmark-Nielsen & Kjær (2003), Svendsen et al. (2015) and Larsen et al. (2009), this period saw the disintegration of the Norwegian Channel Ice Stream (NCIS) in its final stages, which had prior to this significantly contributed to discharging large amounts of the southwestern SIS into the Norwegian Sea. As a result, it is possible that meltwater to a larger extent drained in Skagerrak and Kattegat by 18 ka, which is characterised as a period with rapid deglaciation and deposition in a fjord system (Houmark-Nielsen & Kjær 2003). This freshwater supply and consequent stratification could partly explain the low bottom water $\delta^{13}C$ values during this period.

Kattegat underwent a marine inundation at 17.2 – 17 ka (Houmark-Nielsen 2003; Larsen et al. 2009), establishing marine conditions at the time of the SIS retreat from the basin. It is possible to discern a change around this time, perhaps most clearly in the salinity graph (Figure 13) where a freshening comes to a halt and salinity increases for about half a millennia (from 17.2 to 16.6 ka) before decreasing again. At 16 ka the last ice readvance in eastern Denmark took place, and there was drainage of proglacial lakes and dead ice meltwater into Kattegat. Simultaneously, waters from the Baltic discharged into Kattegat northward through Öresund and Storebelt (Houmark-Nielsen & Kjær 2003). This is expected to be reflected in our record, either as an intense salinity decrease due to an abundance of fresh water supply, or a $\delta^{13}C$ decrease if the drained waters remained on the surface and strengthened stratification. There is only a slight lowering of salinity, but a more distinguished $\delta^{13}C$ decrease (of 1‰) during the three centuries leading up to 15.7 ka. This suggests a final increase in stratification, alternatively a lowering of the $\delta^{13}C$ values due to the arrival of water from the Baltic with a potentially more negative $\delta^{13}C$ signal.

Interestingly, the carbon and oxygen isotope data together reveal what must be an important event at 15.7 ka (21.38 mbsf), where the $\delta^{13}C$ values quickly increase after a long period of stagnant conditions, and the $\delta^{18}O$ shows a salinity increase after a long period of declining salinity. The most dramatic change is seen in the $\delta^{13}C$ record, and there was undoubtedly an occurrence that drove these environmental changes simultaneously. In ~500 years (15.7 – 15.2 ka) the $\delta^{13}C$ values increase by 2.2‰, $\delta^{18}O$ values increase by 1.5‰, and the calculated salinity increases by 5 units. Since stratification and stagnant bottom waters is the most likely reason for the negative $\delta^{13}C$ signal, a change in these conditions probably stems from a mixing event that broke up the salinity stratification and a strong influence of water with more positive $\delta^{13}C$.

If the $\delta^{13}C$ decrease at 16 ka was a result of Baltic water influence, the increase seen at 15.7 ka probably had origins in the North Sea and Atlantic Ocean. Knudsen et al. (1996) interpret a $\delta^{18}O$ and salinity increase in their Skagerrak-Kattegat record as an influence of saline Atlantic bottom water. This, however, occurs much later (13.1 ka) and could not correspond with the 15.7 ka event recorded in our Anholt core, even if the interpretation could be valid. Between 16 and 15 ka, the SIS had retreated to expose considerable areas of southern Sweden and resulted in an ice-dammed lake in the southern Baltic. In Kattegat, sea levels rose and spread southward into the Öresund region. Subsequently, isostatic rebound led to continuous regression in Kattegat, followed by a marine inundation around 15 ka (Houmark-Nielsen & Kjær 2003). The 15.7 ka events recorded by $\delta^{18}O$ and $\delta^{13}C$ are likely to be a result of the increased marine influence in the area.

4.2 Grain size (weight percent coarse fraction)

The early part of the record shows an extremely high sedimentation rate of as much as 4 cm per year,

and the samples from this interval are therefore ultra-high temporal resolution. The cause for this rapid sedimentation is most probably the discharge of sediment-laden glacial meltwater and the calving of glaciers into the basin (Houmark-Nielsen & Kjær 2003). The first two centuries (82.50 – 79.28 mbsf) show coarser grain sizes as the >63µm fraction ranges from ~10 to 30% (Figure 14). This occurs at the same time as the rapid, large freshening interpreted from $\delta^{18}O$. The presence of sand-sized grains suggests that the site was in an ice proximal setting, potentially with icebergs that would have deposited dropstones such as the one found in 80.01 mbsf (18 ka).

After 17.9 ka, the percent coarse fraction decreases sharply and remains low (0% to <7%) until 16.3 ka. The lack of coarse sediments suggests that the ice margin was more distant than before, and few or no icebergs reached this area any longer, but continued rapid sedimentation of silt and clay (Andrén et al. 2015b) suggests that the ice sheet was still relatively near (Knudsen et al. 1996). At 16.3 ka (30 mbsf) the wt. % coarse fraction increases to values between 0 and 10%, and then between 15.9 ka (24 mbsf) and 14.3 ka (9.6 mbsf), values range from 10% to almost 70%. The dramatic increase in grain size at 15.9 ka approximately coincides with changes in the trends of foraminiferal $\delta^{18}O$ and $\delta^{13}C$ at 15.7 ka. Furthermore, the most significant changes in sedimentation rate occur between 16 and 15.7 ka where sedimentation rates of >3 cm/year transition to <0.8 cm/year at the shallow part of the core. The decrease in sedimentation rate coupled with an increase in wt. % coarse fraction suggests that the SIS had retreated significantly and the sediment source transitioned from an ice marginal setting to an environment dominated by sand deposition (Andrén et al. 2015b). Regression is also a possible cause of the change in sediment deposition. The infilling of the Kattegat basin coupled with isostatic rebound would have led to a shallower water depth and consequently a different depositional environment. Besides retreat of the SIS and the resulting regression, the altering of sediment characteristics lend support to Houmark-Nielsen & Kjær's (2003) deglaciation model (Figure 16). By 16 – 15 ka, the southern part of the ice sheet had decayed, leading to meltwater reaching Kattegat from the northeast. The Danish sedimentary glacial flour that had previously made up the bulk of the sediment deposited, was replaced with coarser grains from the hard Fennoscandian crystalline rock.

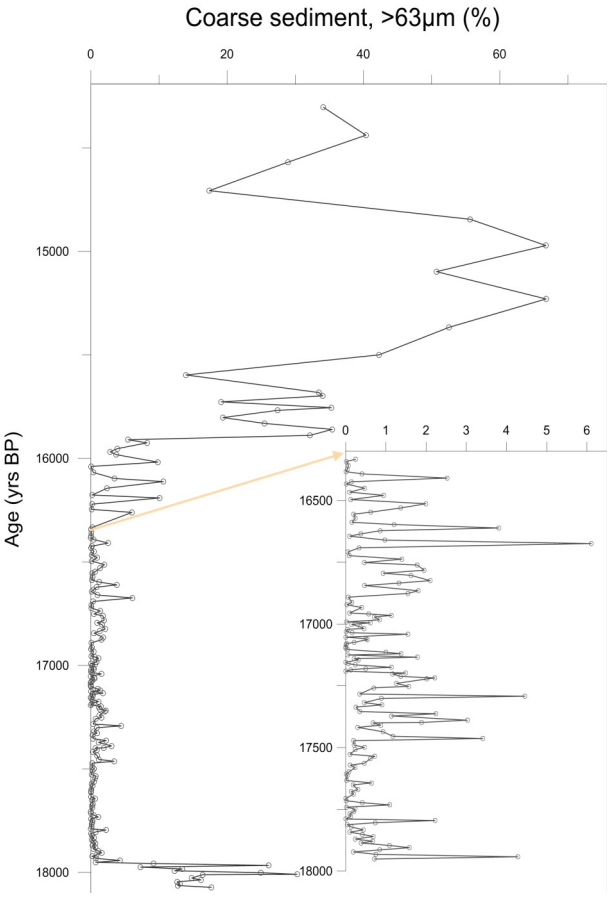

Fig. 14. Weight percent coarse sediment plotted against time, with an inset showing the values close to 0% more clearly. Samples in the oldest and youngest portions of the core have values 10—70%, while most of the record remains between 0 and <7%.

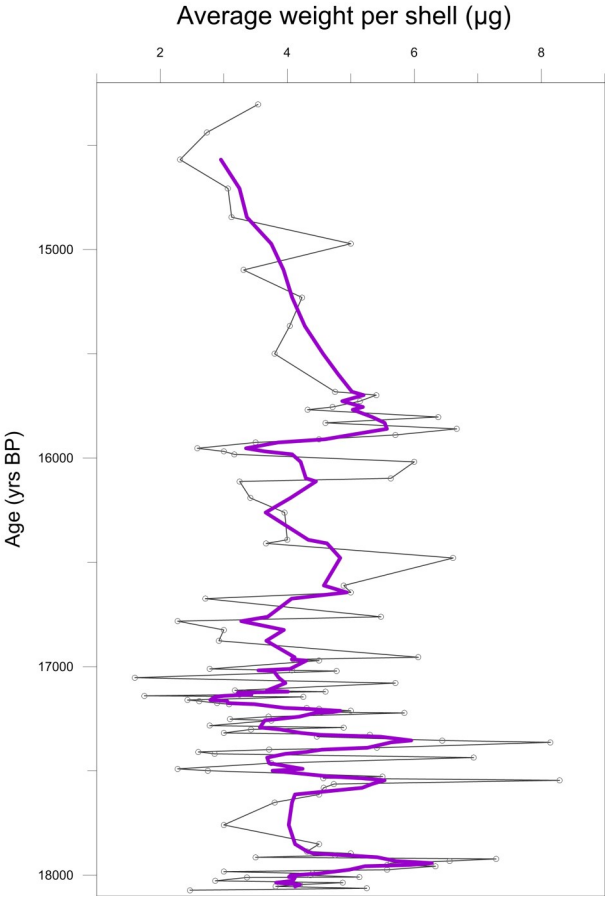

Fig. 15. Average weight per foraminifera shell plotted against age. A 5-point smoothing line has been applied to facilitate discernment of trends, such as the shallow portion which shows a decrease in shell weight.

4.3 Mean shell weight

The average foraminifera shell weight (representing the thickness of the shell) fluctuates between 2 and 8µg from 18.1 to 15.7 ka where it reaches a peak weight of 6µg per shell and then decreases for the rest of the core to ~3µg. The shell thickness can reveal environmental factors, since thicker shelled foraminifera suggest more favourable calcification conditions or a better shell preservation in the sediment. We can assume that after 15.7 ka, conditions became less favourable for *Elphidium excavatum*, alternatively preservation worsened. Being an arctic species, the decreasing shell weight could suggest warming conditions, since *E. excavatum* tolerates a wide salinity range.

Hald et al. (1994) studied the species distribution in arctic seas and concluded that they are most abundant between 1°C and 1.8°C, while almost absent at temperatures higher than 2.5°C. *E. excavatum clavatum* in fjords were found to prefer colder water with reduced salinity and high turbidity. Potentially higher temperatures and salinities in combination with de-

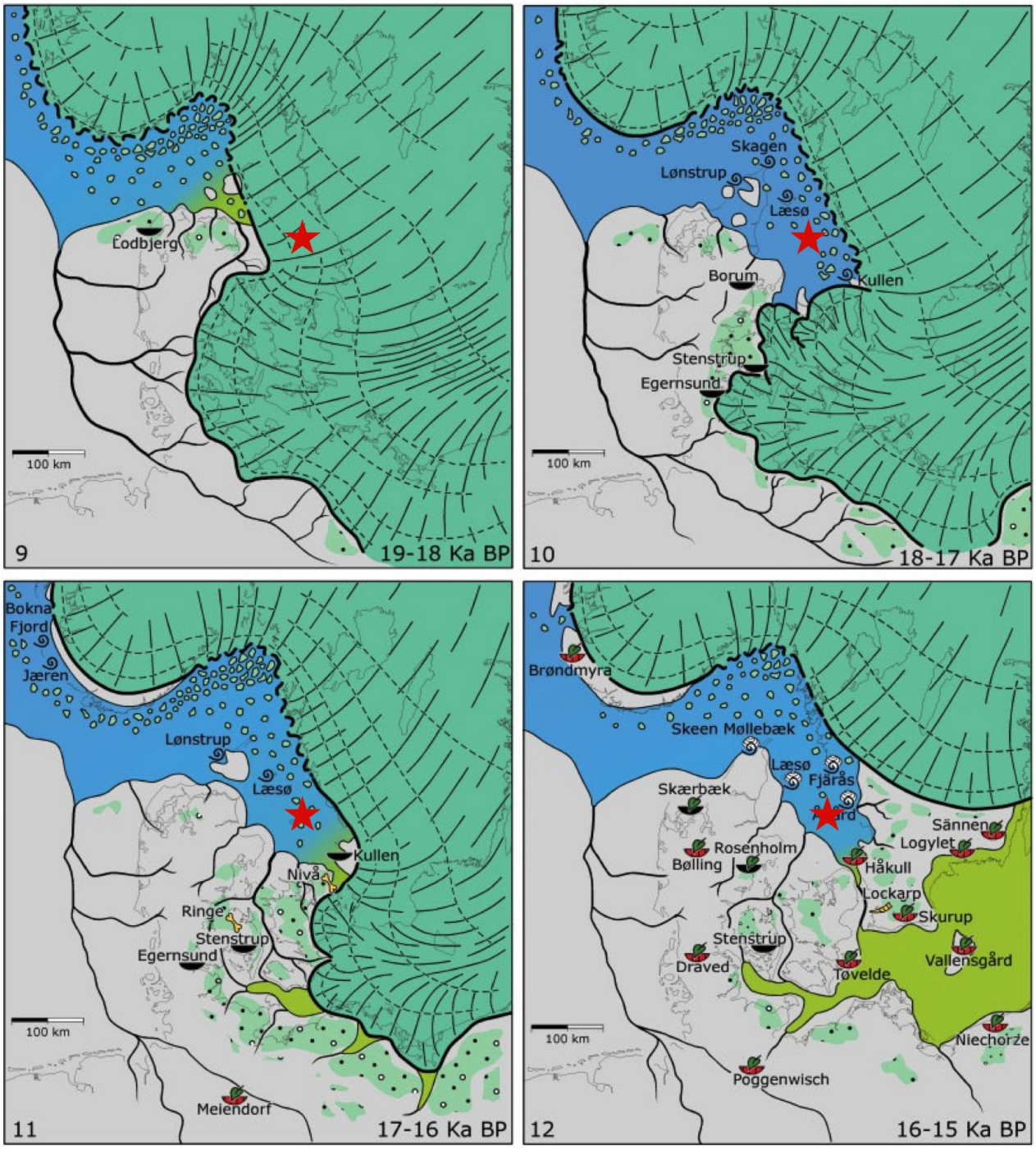

Fig. 16. Paleogeoraphical reconstruction of southwestern Scandinavia during the deglaciation. The maps show the extent of the SIS from 19 to 15 ka. The position of Anholt is marked with a red star. Modified from Houmark-Nielsen & Kjær (2003).

creased turbidity could have caused deteriorating calcification conditions for *E. excavatum.*

4.4 Sources of error

As previously mentioned, there are several different factors that can influence the oxygen and carbon isotope results, and they can be cumbersome to separate. Besides the ambiguities that can arise from attempting to reconstruct paleoenvironments based on non-instrumental proxies, there are also several other potential errors that must be considered before concluding the reliability of interpretations made from these results.

Age model: Creating an age model for any given set of samples is a matter subject to uncertainties. The ages may not be perfectly accurate – fossils could be redeposited or influenced by old carbon, and the reservoir effect subtracted could be wrong. Dating and calibration is performed on a limited number of samples throughout the length of the core and then interpolated to fit each depth. The finished age model therefore gives approximations rather than exact ages. Additionally, each sample is about 2 cm thick, which, depending on the resolution, can represent a few years or a few decades. The small-scale changes are therefore not possible to detect in such an experiment.

Salinity calculations: As already discussed, the sea bottom salinities are based on temperature estimations that may not be accurate enough to give a valid interpretation. The assumption that temperatures have been constant for 3.7 ka, or increased with a constant rate, make salinity calculations reasonable estimations at best or educated guesses at worst. Besides the possibility of having assumed an inappropriate temperature range, none of the equations used have been calibrated for *Elphidium excavatum*, which could also give potential errors, as another foraminifera species is assumed to fractionate identically. The assumptions made when calibrating the paleotemperature calculations are a separate issue that can be further explored by reading the corresponding publications (Epstein et al. 1953; O'Neil et al. 1969; Shackleton 1974; Bemis et al. 1998; Bemis et al. 2002).

Limited proxies: Benthic foraminifera can only be used to record seafloor conditions, but provide no surface water information. Isotope measurements from both benthic and planktonic foraminifera in the same site, would offer a more complete representation of changes in the entire water column. However, no planktic foraminifera occurred in this record, which suggests surface water salinities lower than in the open ocean. Furthermore, foram assemblages have not been analysed for this thesis, which could also improve the data and give a more valid interpretation.

Initial coring: When retrieving a sediment core there is a possibility of limited preservation, as well as sediment expansion and compaction when subjected to changing pressure. Fortunately, the samples presented in this thesis come from core depths where sediment recovery was >90% and only had some minor gaps in the record (Figure 4).

5 Conclusions

The stable isotope, shell weight and grain size records presented in this thesis represent the deglaciation of the late Weichselian (~18 – 14 ka) in the Kattegat. Oxygen isotopes are thought to reflect salinity more than temperature, while $\delta^{13}C$ is interpreted as indicating ventilation, productivity and salinity.

Between 18.0 and 15.7 ka, $\delta^{18}O$ values indicate brackish marine conditions, with a long-term decrease in salinity from nearly marine conditions at 18 ka to increasingly brackish conditions by 15.7. The first couple of centuries of this interval show a rapid freshening of the Kattegat bottom waters followed by a continued, slower salinity decrease until 15.7 ka, with some salinity and/or temperature oscillations during an overall freshening trend. This is interpreted as a period of strong glacial meltwater influence on the Kattegat. Very negative foraminiferal $\delta^{13}C$ values between 18.1 and 15.7 ka suggest stagnant, poorly ventilated, low oxygen bottom waters. This was probably a result of stratification of the water column due to a combination of meltwater-rich surface waters and denser, more saline bottom water in a fjord-like environment.

The weight percent coarse fraction data display a high proportion of coarse sediment at 18 ka, and is interpreted as an ice proximal setting with icebergs. The predominantly silt and clay sediments between 17.9 and 16.3 ka (represented by a low percentage of wt. % coarse fraction) suggests discharge of sediment-laden glacial meltwater and a more distant ice margin and little influence by icebergs. Between16 and 14.3 ka, an increased weight % coarse fraction suggests a change in sediment source and depositional environment.

At 15.7 ka, a large environmental change appears to have occurred, indicated by increased salinity and ventilation (indicated by more positive $\delta^{18}O$ and $\delta^{13}C$), foraminifera shell weight decrease and sedimentation is slower. The increase in salinity could reflect a stronger marine influence due to less fresh water being discharged into the basin from the SIS and more seawater inflow, leading to mixing between the bottom and surface waters and increased ventilation. Although no study specifically identifies 15.7 ka as an important environmental event, these findings agree partially with previous studies that discuss the stages of the deglaciation and their effect on the Kattegat, such as discharge events and influence from the North Sea.

6 Acknowledgements

First and foremost I would like to extend a big thank you to my supervisors Helena L. Filipsson and Nadine B. Quintana Krupinski for their great guidance,

feedback and inspiration. I thank Andreas Mackensen for performing the isotope analyses, Aarno Kotilainen and Outi Hyttinen for providing me with an age model and Karen Luise Knudsen for edifying conversations. I am also grateful to my family in Sweden and Spain for their encouragement and to Jonathan Valerio for his continuous support.

7 References

Allaby, A. & Allaby, M., 1999: *A Dictionary of Earth Sciences.* Oxford University Press.

Alve, E. & Murray, J. W., 1999: Marginal marine environments of the Skagerrak and Kattegat: a baseline study of living (stained) benthic foraminiferal ecology. *Palaeogeography Palaeoclimatology Palaeoecology 146***,** 171-193. doi: 10.1016/s0031-0182(98)00131-x

Andrén, T., Björck, S., Andrén, E., Conley, D., Zillén, L. & Anjar, J. 2011: The development of the Baltic Sea Basin during the last 130 ka. *In The Baltic Sea Basin*, 75-97. Springer,

Andrén, T., Jørgensen, B., Cotterill, C., Green, S., Andrén, E., Ash, J., Bauersachs, T., Cragg, B., Fanget, A. & Fehr, A., 2015: Site M0060. *Proc. IODP| Volume 347.* 2 pp.

Bemis, B. E., Spero, H. J., Bijma, J. & Lea, D. W., 1998: Reevaluation of the oxygen isotopic composition of planktonic foraminifera: Experimental results and revised paleotemperature equations. *Paleoceanography 13***,** 150-160.

Bemis, B. E., Spero, H. J. & Thunell, R. C., 2002: Using species-specific paleotemperature equations with foraminifera: A case study in the Southern California Bight. *Marine Micropaleontology 46***,** 405-430.

Björck, S., 1995: A REVIEW OF THE HISTORY OF THE BALTIC SEA, 13.0-8.0 KA BP. *Quaternary International 27***,** 19-40. doi: 10.1016/1040-6182(94)00057-c

Boersma, A., Haq, B. U. & Boersma, A., 1998: *Foraminifera*. 19-77 pp.

Clark, P. U., Dyke, A. S., Shakun, J. D., Carlson, A. E., Clark, J., Wohlfarth, B., Mitrovica, J. X., Hostetler, S. W. & Mccabe, A. M., 2009: The last glacial maximum. *Science 325***,** 710-714.

Craig, H. 1965: The measurement of oxygen isotope paleotemperatures. *In Stable isotopes in oceanographic studies and paleotemperatures*, 23. Lab. Geol. Nucl Pisa,

Danielssen, D., Edler, L., Fonselius, S., Hernroth, L., Ostrowski, M., Svendsen, E. & Talpsepp, L., 1997: Oceanographic variability in the Skagerrak and northern Kattegat, May–June, 1990. *ICES Journal of Marine Science: Journal du Conseil 54***,** 753-773.

Duplessy, J. C., Shackleton, N. J., Matthews, R. K., Prell, W., Ruddiman, W. F., Caralp, M. & Hendy, C. H., 1984: C-13 record of benthic foraminifera in the last interglacial ocean – implications for the carbon-cycle and the global deep-water circulation. *Quaternary Research 21***,** 225-243. doi: 10.1016/0033-5894(84)90099-1

Epstein, S., Buchsbaum, R., Lowenstam, H. A. & Urey, H. C., 1953: Revised carbonate-water isotopic temperature scale. *Geological Society of America Bulletin 64***,** 1315-1326.

Fairbanks, R. G., Charles, C. D. & Wright, J. D. 1992: Origin of global meltwater pulses. *In Radiocarbon after four decades*, 473-500. Springer,

Farmer, D. M. & Freeland, H. J., 1983: The physical oceanography of fjords. *Progress in oceanography 12***,** 147-219.

Faure, G., 1986: Principles of isotope geochemistry.

Filipsson, H. L. & Nordberg, K., 2010: Variations in organic carbon flux and stagnation periods during the last 2400 years in a Skagerrak fjord basin, inferred from benthic foraminiferal delta 13C. *Geological Society Special Publication 344***,** 261-270. doi: 10.1144/sp344.18

Filipsson, H. L., Nordberg, K. & Gustafsson, M., 2004: Seasonal study of $\delta^{18}O$ and $\delta^{13}C$ in living (stained) benthic foraminifera from two Swedish fjords. *Marine Micropaleontology 53***,** 159-172.

Gyllencreutz, R., Backman, J., Jakobsson, M., Kissel, C. & Arnold, E., 2006: Postglacial palaeoceanography in the Skagerrak. *The Holocene 16***,** 975-985.

Hald, M. & Korsun, S., 1997: Distribution of modern benthic foraminifera from fjords of Svalhard, European Arctic. *Journal of Foraminiferal Research 27***,** 101-122.

Hald, M., Steinsund, P. I., Dokken, T., Korsun, S., Polyak, L. & Aspeli, R., 1994: Recent and Late Quaternary distribution of Elphidium excavatum f. clavatum in arctic seas. *Cushman Foundation for Foraminiferal Research Special Publication 0***,** 141-153.

Houmark-Nielsen, M., 2003: Signature and timing of the Kattegat Ice Stream: onset of the Last Glacial Maximum sequence at the southwestern margin of the Scandinavian Ice Sheet. *Boreas 32***,** 227-241.

Houmark-Nielsen, M. & Henrik Kjær, K., 2003: Southwest Scandinavia, 40–15 kyr BP: palaeogeography and environmental change. *Journal of Quaternary Science 18***,** 769-786.

Katz, M. E., Cramer, B. S., Franzese, A., Hönisch, B., Miller, K. G., Rosenthal, Y. & Wright, J. D., 2010: Traditional and emerging geochemical proxies in foraminifera. *The Journal of Foraminiferal Research 40***,** 165-192.

Knudsen, K. L., Conradsen, K., Heiernielsen, S. & Seidenkrantz, M. S., 1996: Palaeoenviron-

ments in the Skagerrak-Kattegat basin in the eastern North Sea during the last deglaciation. *Boreas 25*, 65-77.

Knudsen, K. L., Eiríksson, J. & Bartels-Jónsdóttir, H. B., 2012: Oceanographic changes through the last millennium off North Iceland: Temperature and salinity reconstructions based on foraminifera and stable isotopes. *Marine Micropaleontology 84*, 54-73.

Lagerlund, E. & Houmark-Nielsen, M., 1993: Timing and pattern of the last deglaciation in the Kattegat region, southwest Scandinavia. *Boreas 22*, 337-347.

Larsen, N. K., Knudsen, K. L., Krohn, C. F., Kronborg, C., Murray, A. S. & Nielsen, O. B., 2009: Late Quaternary ice sheet, lake and sea history of southwest Scandinavia–a synthesis. *boreas 38*, 732-761.

Leppäranta, M. & Myrberg, K., 2009: *Physical oceanography of the Baltic Sea*. Springer Science & Business Media.

Mackensen, A., 2013: High epibenthic foraminiferal $\delta^{13}C$ in the Recent deep Arctic Ocean: Implications for ventilation and brine release during stadials. *Paleoceanography 28*, 574-584.

Mackensen, A., Schumacher, S., Radke, J. & Schmidt, D., 2000: Microhabitat preferences and stable carbon isotopes of endobenthic foraminifera: clue to quantitative reconstruction of oceanic new production? *Marine Micropaleontology 40*, 233-258.

Nordberg, K., 1991: Oceanography in the Kattegat and Skagerrak over the past 8000 years. *Paleoceanography 6*, 461-484.

O'neil, J. R., Clayton, R. N. & Mayeda, T. K., 1969. Oxygen isotope fractionation in divalent metal carbonates. Univ. of Chicago Report.

Park, R. & Epstein, S., 1960: Carbon isotope fractionation during photosynthesis. *Geochimica et Cosmochimica Acta 21*, 110-126. doi: 10.1016/s0016-7037(60)80006-3

Ravelo, A. C. & Hillaire-Marcel, C., 2007: Chapter Eighteen The Use of Oxygen and Carbon Isotopes of Foraminifera in Paleoceanography. *Developments in Marine Geology 1*, 735 -764.

Shackleton, N., 1974: Attainment of isotopic equilibrium between ocean water and the benthonic foraminifera genus Uvigerina: isotopic changes in the ocean during the last glacial.

Svendsen, J. I., Briner, J. P., Mangerud, J. & Young, N. E., 2015: Early break-up of the Norwegian Channel Ice Stream during the Last Glacial Maximum. *Quaternary Science Reviews 107*, 231-242.

Urey, H. C., 1947: The thermodynamic properties of isotopic substances. *Journal of the Chemical Society (Resumed)*, 562-581.

Voipio, A., 1981: *The Baltic Sea*. Elsevier.

Wright, J. D., Miller, K. G. & Fairbanks, R. G., 1991: Evolution of the modern deepwater circulation: evidence from the late Miocene Southern Ocean. *Paleoceanography 6*, 275-290. doi: 10.1029/90pa02498

Zillén, L., Conley, D. J., Andrén, T., Andrén, E. & Björck, S., 2008: Past occurrences of hypoxia in the Baltic Sea and the role of climate variability, environmental change and human impact. *Earth Science Reviews 91*, 77-92.

8 Appendix

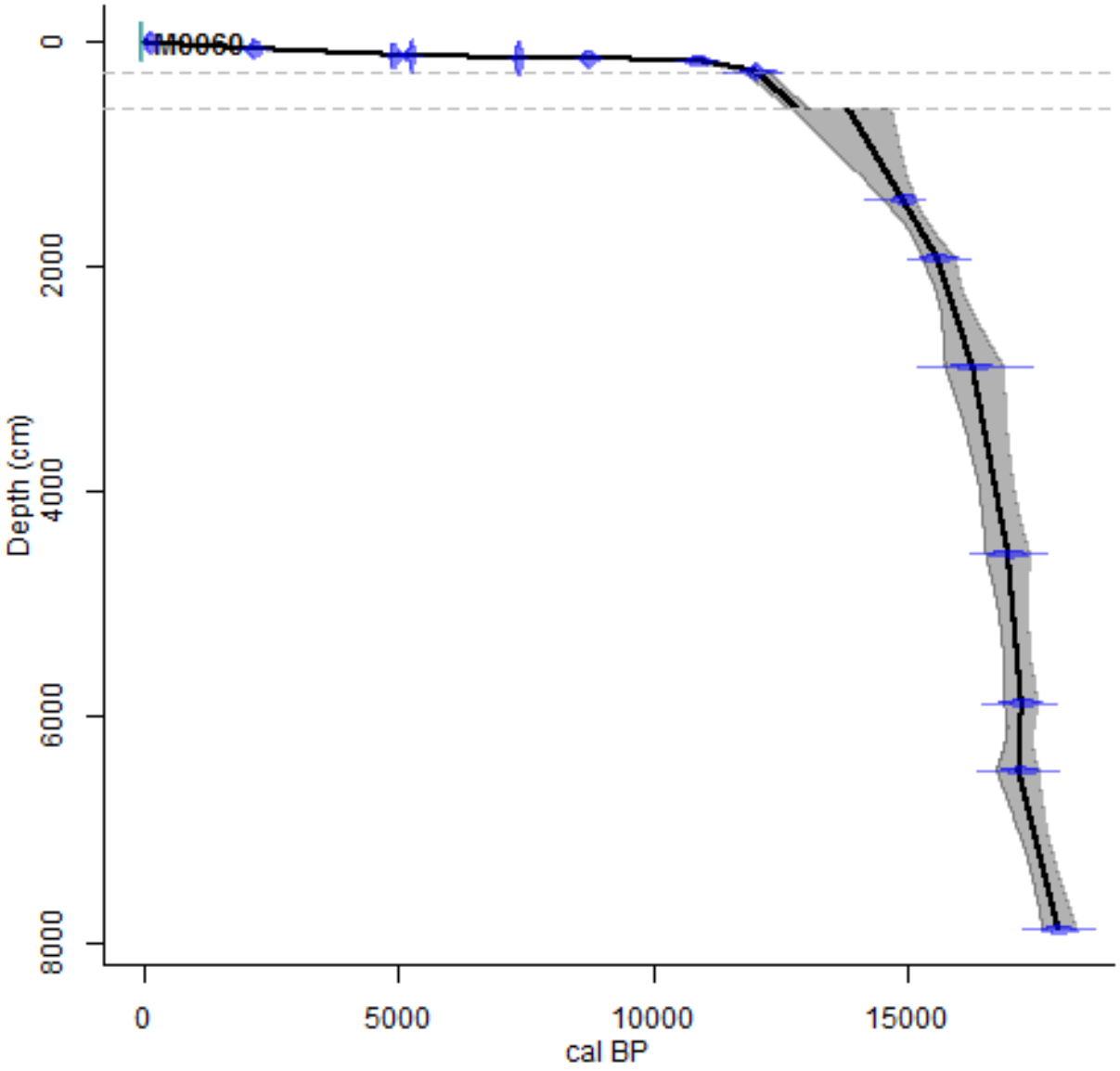

Appendix. 1. Age model for site M0060A. The graph shows calibrated ^{14}C ages for depths down to 80 mbsf. Provided by Aarno Kotilainen and Outi Hyttinen.

Appendix 2: Table with depth, percent coarse fraction (sediment >63µm), average weight per foraminifera shell, oxygen isotope values and carbon isotope values.

Core Section	Top depth (cm)	Bottom depth (cm)	Depth (mbsf)	Sediment >63µm (%)	Avg weight per shell (µg)	$\delta^{18}O$ (‰)	$\delta^{13}C$ (‰)
8 - 1	62	64	9.62	34.12	3.5	-0.497	-1.643
8 - 2	14	16	10.64	40.36	2.7	0.550	-2.181
8 - 2	113	115	11.63	28.95	2.3	-0.329	-2.146
9 - 1	37	39	12.67	17.39	3.1	0.608	-2.222
9 - 1	142	144	13.72	55.65	3.1	0.217	-2.078
9 - 2	88	90	14.68	66.77	5.0	0.446	-2.146
10 - 1	3	5	15.63	50.73	3.3	0.864	-2.197
10 - 1	103	105	16.63	66.80	4.2	-0.100	-1.543
10 - 2	56	58	17.67	52.56	4.0	0.183	-2.117
10 - 3	7	9	18.68	42.29	3.8	0.343	-2.365
11 - 1	67	69	19.57	13.95	6.0	0.666	-2.663
11 - 2	36	38	20.76	33.47	4.8	0.258	-2.416
11 - 2	57	59	20.97	34.02	5.4	-0.016	-2.606
11 - 2	98	100	21.38	19.12	5.1	-0.785	-3.707
11 - 2	137	139	21.77	35.29	4.7	-0.311	-2.959
11 - 3	5	7	21.95	27.40	4.3	0.137	-3.707
12 - 1	24	26	22.44	19.37	6.4	-0.375	-2.981
12 - 1	64	66	22.84	25.49	4.6	-0.113	-3.009
12 - 1	104	106	23.24	35.41	6.7	-0.409	-3.094
12 - 1	144	146	23.64	32.15	5.7	0.056	-3.103
12 - 2	24	26	23.94	5.46	4.5	-0.164	-3.188
12 - 2	44	46	24.14	8.25	3.5	0.054	-2.602
12 - 2	84	86	24.54	3.88	2.6	-0.352	-3.057
12 - 2	105	107	24.75	2.82	3.0	-0.147	-2.932
12 - 2	124	126	24.94	3.74	3.2	0.490	-2.926
12 - 3	24	26	25.44	9.82	6.0	-0.440	-2.766
13 - 1	24	26	25.74	0.02			
13 - 1	64.5	66	26.15	0.36			
13 - 1	105	107	26.55	3.46	5.6	0.125	-2.892
13 - 1	125	127	26.75	10.63	3.3	0.660	-2.920
13 - 2	20	22	27.20	2.38			
13 - 2	66	68	27.66	0.19			
13 - 2	86	88	27.86	10.10	3.4	-0.377	-2.580
13 - 2	128	130	28.28	0.20			
13 - 3	13	15	28.63	0.10			

Core Section	Top depth (cm)	Bottom depth (cm)	Depth (mbsf)	Sediment >63µm (%)	Avg weight per shell (µg)	$\delta^{18}O$ (‰)	$\delta^{13}C$ (‰)
13 - 3	34	36	28.84	6.02	4.0	-0.078	-2.671
15 - 1	6	8	30.56	0.25			
15 - 1	26	28	30.76	0.02			
15 - 1	66	68	31.16	0.07			
15 - 1	106	108	31.56	0.04			
15 - 1	126	128	31.76	0.01			
15 - 1	146	148	31.96	0.41	4.0	0.147	-2.902
15 - 2	37	39	32.37	2.52	3.7	-0.120	-3.306
15 - 2	74	76	32.74	0.14			
15 - 2	96	98	32.96	0.02			
15 - 2	136	138	33.36	0.47			
15 - 3	24	26	33.74	0.10			
16 - 1	27	29	34.07	0.94	6.6	0.502	-2.766
16 - 1	67	69	34.47	0.13			
16 - 1	108	110	34.88	1.99			
16 - 1	148	150	35.28	1.37			
16 - 2	38	40	35.68	0.62			
16 - 2	58	60	35.88	0.20			
16 - 2	98	100	36.28	0.24			
16 - 2	138	140	36.68	0.16			
16 - 3	8	10	36.88	1.20			
17 - 1	13	15	37.23	3.80	4.9	1.495	-2.666
17 - 1	39	41	37.49	0.86			
17 - 1	71	73	37.81	0.38			
17 - 1	91	93	38.01	0.10	5.0	0.903	-2.598
17 - 1	131	133	38.41	0.97			
17 - 2	14	16	38.74	6.11	2.7	0.744	-2.817
17 - 2	55.5	55.7	39.16	0.34			
17 - 2	95	97	39.55	0.06			
17 - 2	132	134	39.92	0.09			
17 - 3	14	16	40.24	1.40			
18 - 1	18	20	40.58	0.46			
18 - 1	43	45	40.83	1.78	5.5	1.161	-2.684
18 - 1	92	94	41.32	1.95	2.3	0.399	-2.565
18 - 1	122	124	41.62	0.93			
18 - 1	143	145	41.83	1.63			
18 - 2	43	45	42.33	2.10	3.0	1.545	-2.713

Core Section	Top depth (cm)	Bottom depth (cm)	Depth (mbsf)	Sediment >63µm (%)	Avg weight per shell (µg)	$\delta^{18}O$ (‰)	$\delta^{13}C$ (‰)
18 - 2	68	70	42.58	1.33			
18 - 2	92	94	42.82	0.47			
18 - 2	142	144	43.32	1.81			
18 - 3	18	20	43.58	1.55	2.9	0.317	-2.834
19 - 1	25	27	43.95	0.07			
19 - 1	75	77	44.45	0.16			
19 - 1	98	100	44.68	0.03			
19 - 1	125	127	44.95	0.40			
19 - 2	27	29	45.47	0.10	6.1	0.503	-2.482
19 - 2	50	52	45.70	0.57			
19 - 2	79	81	45.99	1.14	4.1	0.580	-3.272
19 - 2	108	110	46.28	0.71	4.5	1.034	-2.491
19 - 3	17	19	46.87	0.84			
20 - 1	25	27	47.25	0.03			
20 - 1	47.5	49.5	47.48	0.61			
20 - 1	75	77	47.75	0.15			
20 - 1	125	127	48.25	0.36	2.8	0.513	-3.450
20 - 2	12.5	14.5	48.63	0.46	4.1	0.662	-2.963
20 - 2	25	27	48.75	0.04	4.8	0.909	-3.069
20 - 2	75	77	49.25	0.02			
20 - 2	98	100	49.48	0.16			
20 - 2	124.5	126.5	49.75	1.55			
21 - 1	5	7	50.35	0.01	1.6		
21 - 1	37	39	50.67	0.50			
21 - 1	54	56	50.84	0.54			
21 - 1	108	110	51.38	0.21			
21 - 1	133	135	51.63	0.02	5.7	0.435	-2.991
21 - 2	5	7	51.85	0.01			
21 - 2	55	57	52.35	0.00			
21 - 2	81	83	52.61	0.00			
21 - 2	106	108	52.86	0.05			
21 - 3	10	12	53.40	1.00	3.2	0.595	-2.594
22 - 1	7	9	53.67	1.38	4.6	0.790	-2.769
22 - 1	32	34	53.92	0.05	3.3	1.535	-2.239
22 - 1	81	83	54.41	1.78	3.3	1.148	-2.334
22 - 1	107	109	54.67	0.21	1.8		
22 - 1	132	134	54.92	0.32	4.3	0.724	-3.045

Core Section	Top depth (cm)	Bottom depth (cm)	Depth (mbsf)	Sediment >63µm (%)	Avg weight per shell (µg)	$\delta^{18}O$ (‰)	$\delta^{13}C$ (‰)
22 - 2	31	33	55.41	0.00			
22 - 2	57	59	55.67	0.07	2.4	0.208	-4.082
22 - 2	83	85	55.93	0.24	2.6	0.414	-3.375
22 - 2	131	133	56.41	1.14	2.9	0.585	-2.650
22 - 3	7	9	56.66	0.50	3.1	0.633	-2.809
22 - 3	32	34	56.91	0.12			
23 - 1	35	37	57.25	0.00			
23 - 1	68	70	57.58	1.49	4.3	0.663	-2.508
23 - 1	85	87	57.75	1.17	4.5	0.420	-3.361
23 - 1	135	137	58.25	1.37	5.0	1.657	-2.842
23 - 2	17	19	58.57	2.22	4.5	1.273	-2.476
23 - 2	35	37	58.75	2.02	5.8	1.563	-2.743
23 - 2	85	87	59.25	1.26	3.7	0.991	-2.785
23 - 2	118	120	59.58	1.57	3.1	0.466	-3.423
23 - 2	135	137	59.75	0.70	3.8	1.236	-2.516
24 - 1	25	27	60.45	0.35	2.8	1.234	-2.606
24 - 1	50	52	60.70	4.46	4.9	0.623	-3.355
24 - 1	75	77	60.95	0.89	3.4		
24 - 1	124	126	61.44	0.46	3.0	1.903	-2.210
24 - 2	0	2	61.70	0.90	5.3	1.187	-2.461
24 - 2	25	27	61.95	0.26	4.5	0.896	-3.199
24 - 2	75	77	62.45	0.35	6.4	1.077	-2.693
24 - 2	100	102	62.70	2.25	8.1	1.275	-2.729
24 - 2	124	126	62.94	1.14			
24 - 3	24	26	63.44	3.03	5.4	1.138	-2.691
24 - 4	4	6	63.67	1.89	3.7	1.173	-3.503
25 - 1	25	27	63.75	0.68			
25 - 1	50	52	64.00	0.87	2.6		
25 - 1	75	77	64.25	0.30	2.9	0.616	-2.834
25 - 1	125	127	64.75	0.93	6.9	1.052	-3.415
25 - 2	25	27	65.25	1.17			
25 - 2	50	52	65.50	3.41	3.8		
25 - 2	75	77	65.75	0.20			
25 - 2	125	127	66.25	0.21	2.3	1.529	-3.899
25 - 3	2	4	66.52	0.47	2.8	1.150	-2.652
25 - 3	27	29	66.77	0.24			
26 - 1	50	52	67.30	0.11	5.5	1.391	-3.180

Core Section	Top depth (cm)	Bottom depth (cm)	Depth (mbsf)	Sediment >63µm (%)	Avg weight per shell (µg)	$\delta^{18}O$ (‰)	$\delta^{13}C$ (‰)
26 - 1	73	75	67.53	0.72	4.6	1.118	-4.415
26 - 1	100	102	67.80	0.61	8.3	1.424	-2.901
26 - 2	0	2	68.30	0.47	4.7	1.037	-3.112
26 - 2	22	24	68.52	0.11			
26 - 2	50	52	68.80	0.24	4.6	1.256	-3.583
26 - 2	100	102	69.30	0.08			
26 - 2	123	125	69.53	0.02			
26 - 3	10	12	69.70	0.04	4.5	1.652	-2.980
27 - 1	48	50	70.28	0.02			
27 - 1	75	77	70.55	0.64			
27 - 1	98	100	70.78	0.18	3.8	1.567	-2.738
27 - 2	0	2	71.30	0.31			
27 - 2	24	26	71.54	0.14			
27 - 2	50	52	71.80	0.20			
27 - 2	100	102	72.30	0.00			
27 - 2	126	128	72.56	0.02			
28 - 1	0	2	72.80	0.42			
28 - 1	23	25	73.03	1.10			
28 - 1	48	50	73.28	0.03			
28 - 1	73	75	73.53	0.23			
28 - 1	100	102	73.80	0.21	3.0	1.207	-3.157
28 - 1	121	123	74.01	0.10			
28 - 2	5	7	74.35	0.13			
28 - 2	33	35	74.63	0.00			
28 - 2	50	52	74.80	2.22			
28 - 2	75	77	75.05	0.73			
28 - 2	99	101	75.29	0.04			
28 - 2	123	125	75.53	0.14			
29 - 1	6	8	75.86	0.44			
29 - 1	31	33	76.11	0.11			
29 - 1	57.5	59.5	76.38	0.42	4.5	1.468	-2.363
29 - 1	84	86	76.64	0.68			
29 - 1	110	112	76.90	0.24			
29 - 1	135	137	77.15	0.67			
29 - 2	7	9	77.37	0.38	4.3	0.887	-3.160
29 - 2	34	36	77.64	1.09	5.0	0.980	-2.713
29 - 2	60	62	77.90	1.59	4.8	0.810	-2.212

Core Section	Top depth (cm)	Bottom depth (cm)	Depth (mbsf)	Sediment >63µm (%)	Avg weight per shell (µg)	$\delta^{18}O$ (‰)	$\delta^{13}C$ (‰)
29 - 2	83	85	78.13	0.85	3.5	1.952	-3.361
29 - 2	107.5	109.5	78.38	0.19	7.3	1.357	-3.598
29 - 2	134	136	78.64	0.75	6.6	1.133	-3.324
29 - 3	7	9	78.87	4.28	5.6	0.988	-3.378
29 - 3	32	34	79.12	0.71	5.6	0.753	-3.615
30 - 1	18	20	79.28	9.20	6.3	1.371	-3.111
30 - 1	43	45	79.53	26.07			
30 - 1	68	70	79.78	7.31	5.6	2.417	-2.465
30 - 1	93	95	80.03	13.40	3.0	2.440	-2.816
30 - 1	118	120	80.28	12.29	4.4	1.794	-2.882
30 - 1	143	145	80.53	24.93	4.4	2.860	-2.637
30 - 3	4	6	80.76	30.26	5.1	2.491	-2.462
30 - 3	29	31	81.01	16.40	3.4	2.403	-2.226
30 - 3	54	56	81.26	14.80	2.9	2.495	-2.788
30 - 3	79	81	81.51	16.16	4.9	3.309	-2.397
30 - 3	104	106	81.76	12.67	4.2	2.263	-2.881
30 - 3	129	131	82.01	13.05	3.8	1.614	-3.078
30 - 4	3.5	5.5	82.26	12.77	5.3	2.492	-2.852
30 - 4	28	30	82.50	17.68	2.5	2.449	-2.863

Tidigare skrifter i serien "Examensarbeten i Geologi vid Lunds universitet":

411. Fullerton, Wayne, 2014: REE mineralisation and metasomatic alteration in the Olserum metasediments. (45 hp)
412. Mekhaldi, Florian, 2014: The cosmic-ray events around AD 775 and AD 993 - Assessing their causes and possible effects on climate. (45 hp)
413. Timms Eliasson, Isabelle, 2014: Is it possible to reconstruct local presence of pine on bogs during the Holocene based on pollen data? A study based on surface and stratigraphical samples from three bogs in southern Sweden. (45 hp)
414. Hjulström, Joakim, 2014: Bortforsling av kaxblandat vatten från borrningar via dagvattenledningar: Riskanalys, karaktärisering av kaxvatten och reningsmetoder. (45 hp)
415. Fredrich, Birgit, 2014: Metadolerites as quantitative P-T markers for Sveconorwegian metamorphism, SW Sweden. (45 hp)
416. Alebouyeh Semami, Farnaz, 2014: U-Pb geochronology of the Tsineng dyke swarm and paleomagnetism of the Hartley Basalt, South Africa – evidence for two separate magmatic events at 1.93-1.92 and 1.88-1.84 Ga in the Kalahari craton. (45 hp)
417. Reiche, Sophie, 2014: Ascertaining the lithological boundaries of the Yoldia Sea of the Baltic Sea – a geochemical approach. (45 hp)
418. Mroczek, Robert, 2014: Microscopic shock-metamorphic features in crystalline bedrock: A comparison between shocked and unshocked granite from the Siljan impact structure. (15 hp)
419. Balija, Fisnik, 2014: Radon ett samhällsproblem - En litteraturstudie om geologiskt sammanhang, hälsoeffekter och möjliga lösningar. (15 hp)
420. Andersson, Sandra, 2014: Undersökning av kalciumkarbonatförekomsten i infiltrationsområdet i Sydvattens vattenverk, Vombverket. (15 hp)
421. Martin, Ellinor, 2014: Chrome spinel grains from the Komstad Limestone Formation, Killeröd, southern Sweden: A high-resolution study of an increased meteorite flux in the Middle Ordovician. (45 hp)
422. Gabrielsson, Johan, 2014: A study over Mg/Ca in benthic foraminifera sampled across a large salinity gradient. (45 hp)
423. Ingvaldson, Ola, 2015: Ansvarsutredningar av tre potentiellt förorenade fastigheter i Helsingborgs stad. (15 hp)
424. Robygd, Joakim, 2015: Geochemical and palaeomagnetic characteristics of a Swedish Holocene sediment sequence from Lake Storsjön, Jämtland. (45 hp)
425. Larsson, Måns, 2015: Geofysiska undersökningsmetoder för geoenergisystem. (15 hp)
426. Hertzman, Hanna, 2015: Pharmaceuticals in groundwater - a literature review. (15 hp)
427. Thulin Olander, Henric, 2015: A contribution to the knowledge of Fårö's hydrogeology. (45 hp)
428. Peterffy, Olof, 2015: Sedimentology and carbon isotope stratigraphy of Lower–Middle Ordovician successions of Slemmestad (Oslo-Asker, Norway) and Brunflo (Jämtland, Sweden). (45 hp)
429. Sjunnesson, Alexandra, 2015: Spårämnesförsök med nitrat för bedömning av spridning och uppehållstid vid återinfiltrationav grundvatten. (15 hp)
430. Henao, Victor, 2015: A palaeoenvironmental study of a peat sequence from Iles Kerguelen (49° S, Indian Ocean) for the Last Deglaciation based on pollen analysis. (45 hp)
431. Landgren, Susanne, 2015: Using calcein-filled osmotic pumps to study the calcification response of benthic foraminifera to induced hypoxia under *in situ* conditions: An experimental approach. (45 hp)
432. von Knorring, Robert, 2015: Undersökning av karstvittring inom Kristianstadsslättens NV randområde och bedömning av dess betydelse för grundvattnets sårbarhet. (30 hp)
433. Rezvani, Azadeh, 2015: Spectral Time Domain Induced Polarization - Factors Affecting Spectral Data Information Content and Applicability to Geological Characterization. (45 hp)
434. Vasilica, Alexander, 2015: Geofysisk karaktärisering av de ordoviciska kalkstensenheterna på södra Gotland. (15 hp)
435. Olsson, Sofia, 2015: Naturlig nedbrytning av klorerade lösningsmedel: en modellering i Biochlor baserat på en fallstudie. (15 hp)
436. Huitema, Moa, 2015: Inventering av föroreningar vid en brandövningsplats i

Linköpings kommun. (15 hp)

437. Nordlander, Lina, 2015: Borrningsteknikens påverkan vid provtagning inför dimensionering av formationsfilter. (15 hp)
438. Fennvik, Erik, 2015: Resistivitet och IP-mätningar vid Äspö Hard Rock Laboratory. (15 hp)
439. Pettersson, Johan, 2015: Paleoekologisk undersökning av Triberga mosse, sydöstra Öland. (15 hp)
440. Larsson, Alfred, 2015: Mantelplymer - realitet eller *ad hoc*? (15 hp)
441. Holm, Julia, 2015: Markskador inom skogsbruket - jordartens betydelse (15 hp)
442. Åkesson, Sofia, 2015: The application of resistivity and IP-measurements as investigation tools at contaminated sites - A case study from Kv Renen 13, Varberg, SW Sweden. (45 hp)
443. Lönsjö, Emma, 2015: Utbredningen av PFOS i Sverige och världen med fokus på grundvattnet – en litteraturstudie. (15 hp)
444. Asani, Besnik, 2015: A geophysical study of a drumlin in the Åsnen area, Småland, south Sweden. (15 hp)
445. Ohlin, Jeanette, 2015: Riskanalys över pesticidförekomst i enskilda brunnar i Sjöbo kommun. (15 hp)
446. Stevic, Marijana, 2015: Identification and environmental interpretation of microtextures on quartz grains from aeolian sediments - Brattforsheden and Vittskövle, Sweden. (15 hp)
447. Johansson, Ida, 2015: Is there an influence of solar activity on the North Atlantic Oscillation? A literature study of the forcing factors behind the North Atlantic Oscillation. (15 hp)
448. Halling, Jenny, 2015: Inventering av sprickmineraliseringar i en del av Sorgenfrei-Tornquistzonen, Dalby stenbrott, Skåne. (15 hp)
449. Nordas, Johan, 2015: A palynological study across the Ordovician Kinnekulle. (15 hp)
450. Åhlén, Alexandra, 2015: Carbonatites at the Alnö complex, Sweden and along the East African Rift: a literature review. (15 hp)
451. Andersson, Klara, 2015: Undersökning av slugtestsmetodik. (15 hp)
452. Ivarsson, Filip, 2015: Hur bildades Bushveldkomplexet? (15 hp)
453. Glommé, Alexandra, 2015: $^{87}Sr/^{86}Sr$ in plagioclase, evidence for a crustal origin of the Hakefjorden Complex, SW Sweden. (45 hp)
454. Kullberg, Sara, 2015: Using Fe-Ti oxides and trace element analysis to determine crystallization sequence of an anorthosite-norite intrusion, Älgön SW Sweden. (45 hp)
455. Gustafsson, Jon, 2015: När började plattektoniken? Bevis för plattektoniska processer i geologisk tid. (15 hp)
456. Bergqvist, Martina, 2015: Kan Ölands grundvatten öka vid en uppdämning av de utgrävda dikena genom strandvallarna på Ölands östkust? (15 hp)
457. Larsson, Emilie, 2015: U-Pb baddeleyite dating of intrusions in the southeasternmost Kaapvaal Craton (South Africa): revealing multiple events of dyke emplacement. (45 hp)
458. Zaman, Patrik, 2015: LiDAR mapping of presumed rock-cored drumlins in the Lake Åsnen area, Småland, South Sweden. (15 hp)
459. Aguilera Pradenas, Ariam, 2015: The formation mechanisms of Polycrystalline diamonds: diamondites and carbonados. (15 hp)
460. Viehweger, Bernhard, 2015: Sources and effects of short-term environmental changes in Gullmar Fjord, Sweden, inferred from the composition of sedimentary organic matter. (45 hp)
461. Bokhari Friberg, Yasmin, 2015: The paleoceanography of Kattegat during the last deglaciation from benthic foraminiferal stable isotopes. (45 hp)

LUNDS UNIVERSITET

Geologiska institutionen
Lunds universitet
Sölvegatan 12, 223 62 Lund